The Plant Cell, Vol. 32: 1868–1885, June 2020, www.plantcell.org © 2020 ASPB.



# A Homeotic Mutation Changes Legume Nodule Ontogeny into Actinorhizal-Type Ontogeny

**Defeng Shen,[a,1,2] Ting Ting Xiao,[a,1,3] Robin van Velzen,[a,b] Olga Kulikova,[a] Xiaoyun Gong,[c,4] René Geurts,[a] Katharina Pawlowski,[c] and Ton Bisseling[a,5]**

[a] Laboratory of Molecular Biology, Wageningen University, Graduate School Experimental Plant Sciences, 6708 PB Wageningen, the Netherlands

[b] Biosystematics Group, Department of Plant Sciences, Wageningen University, 6708 PB Wageningen, the Netherlands

[c] Department of Ecology, Environment and Plant Sciences, Stockholm University, 106 91 Stockholm, Sweden

ORCID IDs: 0000-0002-6530-8837 (D.S.); 0000-0003-4166-9483 (T.T.X.); 0000-0002-6444-7608 (R.v.V.); 0000-0002-4887-1185 (O.K.); 0000-0003-1791-9382 (X.G.); 0000-0002-6443-2289 (R.G.); 0000-0003-2693-885X (K.P.); 0000-0001-5494-8786 (T.B.)

**Some plants fix atmospheric nitrogen by hosting symbiotic diazotrophic rhizobia or *Frankia* bacteria in root organs known as nodules. Such nodule symbiosis occurs in 10 plant lineages in four taxonomic orders: Fabales, Fagales, Cucurbitales, and Rosales, which are collectively known as the nitrogen-fixing clade. Nodules are divided into two types based on differences in ontogeny and histology: legume-type and actinorhizal-type nodules. The evolutionary relationship between these nodule types has been a long-standing enigma for molecular and evolutionary biologists. Recent phylogenomic studies on nodulating and nonnodulating species in the nitrogen-fixing clade indicated that the nodulation trait has a shared evolutionary origin in all 10 lineages. However, this hypothesis faces a conundrum in that legume-type and actinorhizal-type nodules have been regarded as fundamentally different. Here, we analyzed the actinorhizal-type nodules formed by *Parasponia andersonii* (Rosales) and *Alnus glutinosa* (Fagales) and found that their ontogeny is more similar to that of legume-type nodules (Fabales) than generally assumed. We also show that in *Medicago truncatula*, a homeotic mutation in the co-transcriptional regulator gene *NODULE ROOT1* (*MtNOOT1*) converts legume-type nodules into actinorhizal-type nodules. These experimental findings suggest that the two nodule types have a shared evolutionary origin.**

## INTRODUCTION

Nitrogen-fixing root nodule symbiosis represents the most efficient biological process by which atmospheric nitrogen is transferred into ammonium and becomes a nitrogen source for plants. Nodules are specialized novel root organs whose formation is triggered by diazotrophic *Frankia* or rhizobium bacteria (reviewed by Sprent et al., 1987; Pawlowski and Bisseling, 1996; Huss-Danell, 1997; Franche et al., 2009; Pawlowski and Demchenko, 2012; Santi et al., 2013; Imanishi et al., 2014; Ibáñez et al., 2017).

Nitrogen-fixing root nodule symbioses occur in 10 paraphyletic lineages in the so-called nitrogen-fixing clade (NFC), which is represented by the orders Fabales, Fagales, Cucurbitales, and Rosales (Soltis et al., 1995; Supplemental Figure 1). Species of the Fabaceae (order Fabales) and the genus *Parasponia* (Cannabaceae, order Rosales) form nodules with rhizobia, whereas the eight lineages of actinorhizal plant species (in the orders Fagales, Cucurbitales, and Rosales) form nodules with *Frankia*. Nodulation is common in the Fabaceae of the order Fabales but rare in the other three orders, which also represent many lineages of nonnodulating species. Recent phylogenomics studies showed that nonnodulating species within the NFC lost some genes that are essential and specific for nodulation (Griesmann, 2018; van Velzen, 2018). Therefore, it has been hypothesized that the nodulation trait evolved in the common ancestor of the NFC and was subsequently lost in many descendant lineages (van Velzen et al., 2019). However, this hypothesis does not readily explain differences in the ontogeny and histology of legume and actinorhizal nodule types, which are considered to be fundamental and suggestive of the independent origins of these structures (Doyle, 2011; Parniske, 2018). To overcome this discrepancy, it has been suggested that the common ancestor of the NFC evolved the capacity to accommodate intracellular bacterial infection only in root cortical cells; thereafter, nodule formation evolved several times independently (Parniske, 2018).

Fate maps are indispensable for comparing developmental programs leading to nodule formation in different lineages. A detailed fate map was constructed for the model legume Medicago (*Medicago truncatula*; Xiao et al., 2014). According to this fate map, cell division is first induced in the root pericycle and then extends to endodermal and inner cortical cells from which a nodule primordium is formed. After a few rounds of cell division, the pericycle- and endodermis-derived cells lose their mitotic activity and form approximately eight layers of cells that are not

[1] These authors contributed equally to this work.

[2] Current address: Department of Plant Microbe Interactions, Max Planck Institute for Plant Breeding Research, 50829 Cologne, Germany

[3] Current address: King Abdullah University of Science and Technology (KAUST), Biological and Environmental Sciences and Engineering (BESE), Thuwal 23955-6900, Saudi Arabia

[4] Current address: Faculty of Biology, Genetics, Ludwig-Maximilians University Munich, 82152 Martinsried, Germany

[5] Address correspondence to ton.bisseling@wur.nl.

The author responsible for distribution of materials integral to the findings presented in this article in accordance with the policy described in the Instructions for Authors (www.plantcell.org) is Ton Bisseling (ton.bisseling@wur.nl).

www.plantcell.org/cgi/doi/10.1105/tpc.19.00739

infected by rhizobia. The cells derived from the inner cortex are penetrated by infection threads that originate in the epidermis and grow toward these cells. At this stage, a noninfected meristem forms from the middle cortical cell layer. Rhizobia are released from infection threads into the cells derived from the inner cortex. Once inside, the bacteria divide and differentiate, leading to a situation where infected plant cells ultimately contain hundreds of nitrogen-fixing rhizobia. These cells will form the infected central tissue, which grows via the addition of cells by the apical meristem. Vascular bundles form at the periphery of the nodule primordium and mainly originate from cells derived from the dividing inner cortical cells; their growth is subsequently controlled by the apical meristem (Xiao et al., 2014). To connect the cortex-derived nodule vasculature with the root vasculature, the pericycle- and endodermis-derived cells at the periphery form a few layers of nodule vasculature at the basal region. A characteristic of all legume nodules investigated to date is that the infected central tissue forms from mitotically activated cortical cells. Furthermore, the vascular bundles are located at the periphery and also mainly form from cortex-derived cells.

Actinorhizal-type nodules, including nodules induced by rhizobium on *Parasponia* spp, are coralloid (coral-shaped) organs consisting of multiple lobes with a central vascular system. These lobes are considered to arise via a modified lateral root developmental program originating in the pericycle (Pawlowski and Bisseling, 1996; Huss-Danell, 1997; Pawlowski and Demchenko, 2012; Svistoonoff et al., 2014; Ibáñez et al., 2017). The nodules of some actinorhizal plants can even contain a root growing out of the lobe apex (Pawlowski and Bisseling, 1996; Franche et al., 2009). The cortical cells of these "modified lateral roots" are thought to be infected without first being mitotically activated (Pawlowski and Bisseling, 1996; Santi et al., 2013). Studies on the initial stages of actinorhizal-type nodule formation in Fagales species have shown that a group of root cortical cells can be mitotically activated and become infected. These so-called prenodules are considered to be important for infection but do not develop into an integral part of the actinorhizal-type nodule (Pawlowski and Bisseling, 1996; Franche et al., 2009; Pawlowski and Demchenko, 2012; Santi et al., 2013; Svistoonoff et al., 2014). In contrast to legumes, however, a detailed developmental fate map of actinorhizal-type nodules is lacking, and our current view on the ontogeny of actinorhizal-type nodules might be incorrect.

Novel organs generally originate through the modification of existing developmental programs (Carroll, 2000; Shubin et al., 2009). Homeotic genes are key players in determining the identity of an organ. A loss-of-function mutation in a homeotic gene can result in a switch to the ancestral developmental program. A classic example in fruit fly (*Drosophila*) species is the switch from halter to wing development in response to mutations in the *Ultrabithorax* gene (Lewis, 1963). In plants, the developmental program of flower organs can (partially) switch to that of (vegetative) leaves by mutating a few homeotic genes (Ditta et al., 2004). In the case of root nodules, a mutation in a homeotic gene may uncover the evolutionary relationship of root lateral organs, including both nodule types. One such gene is *NOOT-BOP-COCH-LIKE* (*NBCL*), encoding a co-transcriptional regulator. Mutations in this gene (named *NODULE ROOT1* [*MtNOOT1*] in Medicago, *COCHLEATIA1* [*PsCOCH1*] in pea [*Pisum sativum*], and *LjNBCL1* in *Lotus japonicus*) can cause root outgrowth from nodules, suggesting that this gene functions in maintaining nodule identity (Couzigou, 2012; Magne et al., 2018b).

Here, we present detailed fate maps for actinorhizal-type nodules formed by Parasponia (*Parasponia andersonii*) and Alnus (*Alnus glutinosa*). The fate maps indicate that the ontogeny of these actinorhizal-type nodules is much more similar to that of legume nodules than generally assumed. Furthermore, we show that a mutation in Medicago *MtNOOT1* converts the ontogeny of legume-type nodules into that of actinorhizal-type nodules. These findings suggest that these two types of nodules have a common evolutionary origin and that legume-type nodules evolved from an actinorhizal-type nodule.

## RESULTS

### Infected Cells in Actinorhizal-Type Nodules Are Derived from the Root Cortex

Actinorhizal-type nodules have been described as being composed of "modified lateral roots" (Pawlowski and Bisseling, 1996; Pawlowski and Demchenko, 2012; Ibáñez et al., 2017). To investigate the extent to which the nodule developmental program is distinct from the lateral root developmental program, we aimed to generate fate maps of two representative species: Parasponia and Alnus. These two species were selected because they can grow in square Petri dishes, allowing for spot inoculation with rhizobia/*Frankia*. This is essential for obtaining young nodule primordia for ontogenetic analysis.

First, we analyzed the ontogeny of lateral roots from Parasponia and Alnus. Sectioning of roots from both species revealed that lateral root primordia are derived from the pericycle and endodermis, as in other plant species including field bindweed (*Convolvulus arvensi*; Bonnett, 1969), carrot (*Daucus carota*; Lloret et al., 1989), and onion (*Allium cepa*; Casero et al., 1996). During lateral root formation, four to six pericycle cells and their adjacent endodermis cells were mitotically activated (Supplemental Figures 2A, 2B, and 3A). Endodermis cells only divided anticlinally (Supplemental Figures 2C to 2E and 3B) and formed the outermost layer of the lateral root primordium and later became part of the root cap/columella (Supplemental Figures 2F and 3C). In the lateral root primordium, the epidermis, cortex, and vasculature surrounded by a newly formed endodermis could be discerned (Supplemental Figures 2F and 3C).

Next, we studied nodule primordium formation by applying a compatible symbiont (*Bradyrhizobium elkanii* WUR3 for Parasponia and *Frankia alni* ACN14a for Alnus) onto in vitro grown plants (see Methods). During the early nodule primordium formation stage, cell divisions occurred in the root cortex and pericycle in both plant species (Figures 1A, 1B, 2A, and 2B). In Parasponia, cell divisions were also induced in the epidermis (Figure 1A). During subsequent stages, cell divisions continued in the cortex, and anticlinal divisions were induced in endodermis cells. In contrast to legume nodule primordium formation, in Parasponia and Alnus, cell division in the pericycle persisted and led to the formation of a dome-shaped structure (Figures 1F and 2D; Supplemental Figure 4A). At a subsequent stage, the

pericycle-derived dome formed vascular tissue and was flanked by cells derived from mitotically activated (parental) root endodermis cells. These cells had lost their Casparian strips and formed a new nodule vascular endodermis. In Parasponia, these nodule vascular endodermis cells regained identity at an early stage by forming new Casparian strips (Figure 1I; Supplemental Figure 4B), whereas in Alnus, such a nodule vascular endodermis formed at a later stage of development (Supplemental Figure 5). Therefore, in both species, the nodular structure that formed from the pericycle was a vasculature flanked by a newly formed endodermis and not a modified lateral root (Figures 1F and 2E). This implies that the pericycle-derived nodular structure does not have a cortex and therefore lacks cells that can be infected by bacteria. Cells that become infected by bacteria are derived from dividing root cortical cells, which will form the infected tissue of the nodule (Figures 1F and 2E). At the apex of the pericycle-derived vasculature, endodermis-derived cells lacked Casparian strips and appeared to remain mitotically active (Figures 1J, 1L, and 2J; Supplemental Figure 4C). A group of dividing cells at the tip of the vasculature appeared to form a nodule meristem. The nodule meristem supported the growth of the nodule vascular bundle and added cells to the cortex-derived infected cells (Figures 1K and 2G).

Taken together, these observations indicate that in Parasponia as well as Alnus, cells derived from the root cortex form the infected tissue, and the prenodule becomes part of the mature nodule. The finding that mitotically activated root cortex cells form the infected tissue is similar to that of legume nodule formation. However, in contrast to legume-type nodules, where the nodule vasculature is formed by cortex-derived cells, in actinorhizal-type nodules of Alnus and Parasponia, the nodule vasculature is derived from pericycle cells. Therefore, a key difference between legume and Alnus/Parasponia nodules is the origin of the vasculature, i.e., the cortex in legumes and the pericycle in actinorhizal-type nodules.

To determine whether the nodule ontogeny observed in Alnus and Parasponia holds true for the nodules of other actinorhizal plant species, we carefully reinterpreted published data (Torrey, 1976; Callaham and Torrey, 1977; Torrey and Callaham, 1979; Newcomb and Pankhurst, 1982; Hafeez et al., 1984; Lancelle and Torrey, 1984, 1985; Miller and Baker, 1985; Burgess and Peterson, 1987; Racette and Torrey, 1989; Liu and Berry, 1991; Berg et al., 1999; Valverde and Wall, 1999; Fournier, 2018). The developmental fate of root endodermis cells was not traced in any of these studies. Consequently, it could not be determined whether pericycle-derived cells solely contribute to the formation of nodule vasculature and do not form a cortical tissue that can be infected by the nitrogen-fixing microbe. Therefore, none of these studies provided direct support for the assumption that actinorhizal-type nodules are composed of "modified lateral roots," which would mean that functional nodules would have the exact same origin as lateral roots.

In the order Fagales, in addition to Alnus, *Comptonia peregrina*, *Myrica gale*, and *Casuarina cunninghamiana* have been shown to form infected prenodules derived from root cortical cells (Torrey, 1976; Callaham and Torrey, 1977; Torrey and Callaham, 1979). This opens the possibility that the nodule ontogeny observed in Alnus/Parasponia is a common trait in this order. In Rosales, in addition to Parasponia, cortical cell divisions were also observed in *Ceanothus arboreus*, but the infection of these cells was not reported (Liu and Berry, 1991). Whether cell divisions in Cucurbitales species are induced in root cortical cells has not been investigated (Newcomb and Pankhurst, 1982; Hafeez et al., 1984; Berg et al., 1999). Nevertheless, the occurrence of the Alnus/Parasponia nodule type in a wide range of Fagales species and in two Rosales species is most consistent with the idea that their common ancestor, so also the ancestor of Cucurbitales species, formed this actinorhizal-type nodule. A common feature of actinorhizal-type nodule development is that pericycle-derived cells form the nodule vasculature (Figures 1F, 2E, 5B, and 5D [Figure 5 is a summary of Figures 1 to 4]). This is a major difference from legume-type nodules, where the nodule vasculature is derived from the root cortex (Figure 5F; Xiao et al., 2014). As the nodule vasculature of actinorhizal-type nodules most likely has an identity that is closer to that of a lateral root, this might explain why the apical meristems of lobes of some actinorhizal-type nodules can spontaneously start forming roots at the apex of nodule lobes (Pawlowski and Bisseling, 1996; Franche et al., 2009).

### Medicago *MtNOOT1* Functions as a Homeotic Gene Controlling Legume-Type Nodule Ontogeny

The finding that in both actinorhizal-type and legume-type nodules the infected tissue is derived from mitotically activated root cortical cells suggests they might have a common evolutionary origin. To investigate this notion, we searched for a legume mutant with the ability to form roots at the apex of nodules. We selected a legume with a mutation in the *NOOT/NBCL* gene, which can form functional nodules and, like some actinorhizal-type nodules, can form a root at their apex (Couzigou, 2012; Magne et al., 2018a). To determine if the vascular bundles in *noot/nbcl* mutant nodules have a similar ontogeny to that observed in actinorhizal-type nodules, we studied nodule development in the Medicago *Mtnoot1* knockout mutant.

We compared *Mtnoot1* nodule primordia with wild-type primordia containing inner cortical cells (C4 and C5) at similar developmental stages. We first analyzed *Mtnoot1* nodule primordia when C4 and C5 started to divide. In *Mtnoot1*, pericycle-derived cells formed two layers compared to one layer in wild-type nodule primordia (Figures 3A and 3B). When *Mtnoot1* nodule primordia contained approximately eight cell layers derived from C4 and C5 and the infection threads just reached the inner cortex, there were approximately six to eight cell layers derived from the endodermis and pericycle, whereas only four to six of such cell layers occurred in wild-type nodule primordia (Figures 3C and 3D). At subsequent stages of *Mtnoot1* nodule primordium development, the infection threads formed branches, and the differences between *Mtnoot1* and the wild type became more pronounced. This is because in wild-type nodule primordia, pericycle- and endodermis-derived cells stopped dividing, whereas they remained mitotically active in the *Mtnoot1* mutant (Figures 3E and 3F). In addition, there were fewer cell divisions in the middle cortex (C3) in the *Mtnoot1* mutant compared with the wild type (Figures 3C to 3F). Such changes in the mitotic activities of endodermis/pericycle-derived cells and the C3 layer were observed in the vast majority of *Mtnoot1* nodule primordia (73%, 45/62). We included a second allele of *Mtnoot1* (NF2717) in the analyses. This revealed a similar pattern in the

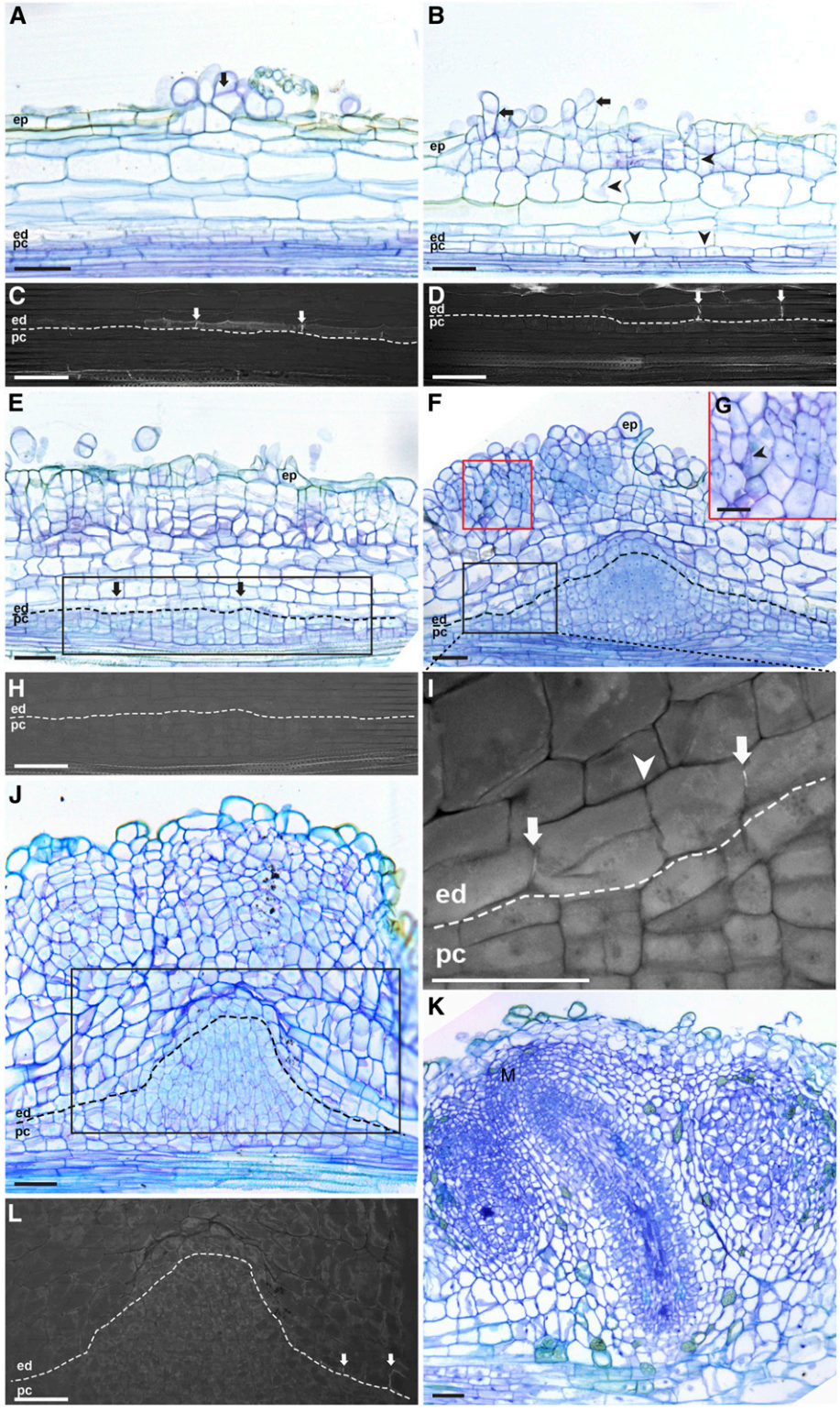


**Figure 1.** Parasponia Root Nodule Developmental Stages.

**(A)** Nodule formation starts with cell divisions in the epidermis (arrow).
**(B)** Cell divisions are induced in the outer cortical cell layers and pericycle (arrowheads), and divisions continue in the epidermis (arrows).

second *Mtnoot1* mutant allele (78%, 40/51; Supplemental Figure 6). Therefore, the gradient of mitotic activity from inner cell layer (pericycle and endodermis) to outer cell layer (C3) is opposite in *Mtnoot1* and wild-type nodule primordia.

In wild-type Medicago nodules, vascular bundles are generated from primordium cells derived from the inner cortex and grow via the activity of the nodule meristem (Xiao et al., 2014). To trace endodermis-derived cells at later stages of development, we introduced the *ProAtCASP1:β-glucuronidase* (*GUS*) reporter into *Mtnoot1* and wild-type roots by *Agrobacterium rhizogenes*-mediated transformation. *AtCASP1* (*CASPARIAN STRIP MEMBRANE DOMAIN PROTEIN1*) is an Arabidopsis (*Arabidopsis thaliana*) gene that is specifically expressed in the root endodermis (Roppolo et al., 2011). The *ProAtCASP1:GUS* reporter is also specifically expressed in the Medicago root endodermis, and during nodule primordium formation, it remains, for some time, expressed in endodermis-derived cells, by which the formation of these cells can be traced (Supplemental Figure 7; Xiao et al., 2014). In *Mtnoot1*, *ProAtCASP1:GUS* was expressed in one to two cell layers surrounding the tips of developing nodule vascular bundles (Figure 4D), implying that these cells were derived from the root endodermis and that the vascular bundles developed from pericycle-derived cells. Therefore, the ontogeny of the *Mtnoot1* nodule vasculature is different from that of the wild type and more similar to that of actinorhizal-type nodules. Mutations in the *MtNOOT1* orthologs of pea (*Pscoch1*) and *L. japonicus* (*Ljnbcl1*) can also cause root outgrowth from nodules (Couzigou, 2012; Magne et al., 2018b). Therefore, we assume that the ontogeny of the nodule vasculature is also actinorhizal-like in these legume mutants. In actinorhizal-type nodules (on plants such as *M. gale* and *Datisca glomerata*), which can form so-called nodule roots, the apical meristems of lobes have the potential to switch to root production (Pawlowski and Bisseling, 1996; Franche et al., 2009). Therefore, it is likely that the potential of legume *noot1/nbcl1* mutant nodules to form nodule roots is caused by their similarity to actinorhizal-type nodules regarding vasculature ontogeny.

## Legume *NOOT/NBCL* Experienced Ancestral Duplications in Two Legume Subfamilies

The loss of function of homeotic genes tends to lead to an ancestral phenotype (Garcia-Bellido, 1977; Wellmer et al., 2014). In line with this observation, we hypothesized that actinorhizal-type nodules are ancestral and that legume-type nodules evolved from these nodules. Legume-specific neofunctionalization of *MtNOOT1-PsCOCH1-LjNBCL1* could have contributed to this switch. Therefore, we explored whether this hypothesis could be supported by the evolutionary trajectory of this gene.

Species of the legume subfamily Papilionoideae generally contain two *NOOT/NBCL* genes, which are grouped in two distinct subclades: the NBCL1 and NBCL2 subclades (Magne et al., 2018a). Medicago *MtNOOT1*, pea *PsCOCH1*, and *L. japonicus LjNBCL1* are orthologs belonging to the NBCL1 subclade (Magne et al., 2018a). Mutant analysis in Medicago demonstrated that only *Mtnoot1* mutant nodules form nodule roots, whereas a mutation in the Medicago *MtNOOT2* gene (of the NBCL2 subclade) does not result in nodules with nodule roots (Magne et al., 2018a). Therefore, the NBCL1 subclade might have contributed to the evolution of the legume-type nodule, and its evolution might have been driven by an ancestral duplication in the NOOT/NBCL orthogroup. To address this notion, we analyzed the phylogeny of *NOOT/NBCL* genes in species within three legume subfamilies for which sequence data are available. The subfamily Cercidoideae is sister to the two other subfamilies, Papilionoideae and Caesalpinioideae (LPWG, 2017). The two species of Cercidoideae, *Cercis canadensis* and *Bauhinia tomentosa*, do not form nodules and contain a single *NOOT/NBCL* gene. Almost all other legumes (subfamilies Papilionoideae and Caesalpinioideae) contain two such genes, which are grouped into four major clades, with two clades representing NBCL subclades of Papilionoideae species (e.g., Medicago and pea) and the other two clades representing the *NOOT/NBCL* genes of Caesalpinioideae species (Figure 6). This finding suggests that independent ancestral duplications have occurred in the common ancestor of each legume subfamily.

**Figure 1.** (continued).

**(C)** and **(D)** UV light images of the endodermis regions of the sections shown in **(A)** and **(B)**, respectively, to visualize the fluorescence of Casparian strips. At the site of nodule primordium formation, the Casparian strips of endodermis cells are visible (arrows).

**(E)** Cell divisions occur in all cortical cell layers, pericycle, and the endodermis (arrows).

**(F)** and **(G)** Cortex-derived cells contain rhizobium-induced infection threads (see arrowhead in **[G]**) and the red boxed region in **[F]**). Pericycle-derived cells form a dome-shaped structure flanked by root endodermis-derived cells.

**(H)** and **(I)** UV light images of the root endodermis regions indicated by the black boxes in the sections shown in **(E)** and **(F)**, respectively.

**(H)** Mitotically activated root endodermis cells have lost their Casparian strips.

**(I)** Casparian strips reformed in the peripheral region (arrows; see Supplemental Figure 4B for the right-side region) but are still absent in the central region of root endodermis-derived cells (Supplemental Figure 4C). The root endodermis-derived cells have divided, especially the cells between the two arrows in **(I)**. The Casparian strips are not present at the conjunction site between these two dividing endodermal cells (arrowhead). This implies that these Casparian strips (arrows) are newly formed.

**(J)** Cell divisions continue in the outer cortical cells. The pericycle-derived dome-shaped structure starts to elongate and forms the vascular tissues. At the apex of the pericycle-derived vasculature, endodermis-derived cells have a thinner cell wall and appear to remain mitotically active.

**(K)** The outer cortex-derived cells become part of the mature nodule. A group of dividing cells at the apex of the nodule vasculature appears to form a nodule meristem (M), supporting the growth of the nodule vasculature and adding cells to the infected tissue.

**(L)** UV light image of the root endodermis region of the section shown in **(J)**. Root endodermis-derived cells flanking the pericycle cells have formed Casparian strips (arrows). This is the newly formed endodermis that surrounds the nodule vasculature. Endodermis-derived cells remain undifferentiated at the apex of the pericycle-derived vasculature and appear to maintain mitotic activity. Dotted lines mark the border between endodermis- and pericycle-derived cells. ep, Epidermis; ed, endodermis; pc, pericycle. Scale bars, 50 μm **([A]** to **[F]** and **[H]** to **[L]**), 25 μm **(G)**.

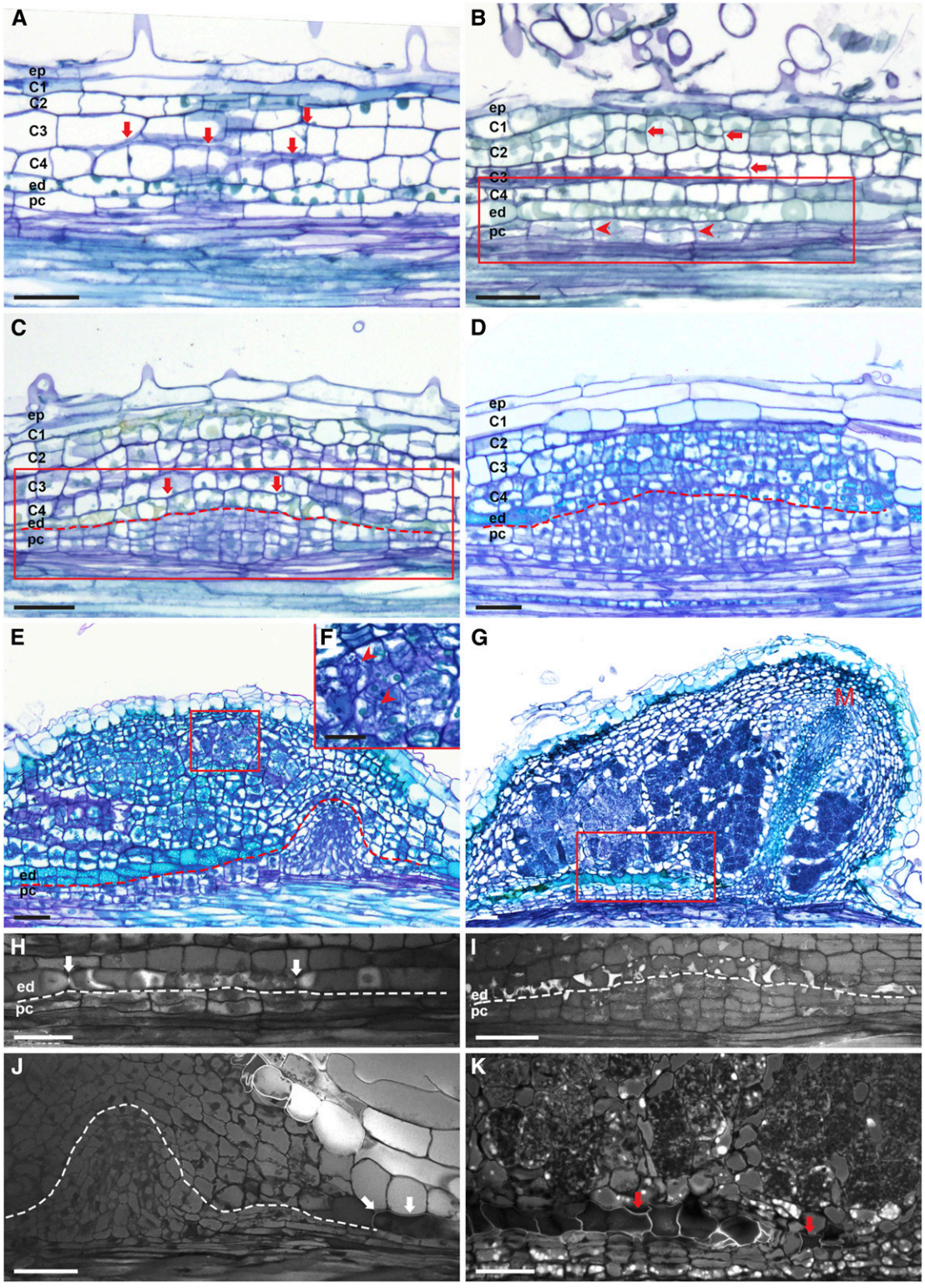


**Figure 2.** Alnus Root Nodule Developmental Stages.

**(A)** Nodule formation starts with anticlinal divisions in the cortex (arrows).
**(B)** and **(H)** Subsequently, divisions are induced in the pericycle (arrowheads) and continue in the cortex (arrows). **(H)** UV light image of the endodermis region of the section shown in **(B)**. Not yet divided endodermis cells still have Casparian strips (arrows).

To confirm this notion, we conducted microsynteny analysis of *NOOT/NBCL* genes in legumes and compared them with genes from several other rosid species. We selected species with a single *NOOT/NBCL* gene because they could contain a rather conserved microsyntenic block, whereas duplication tends to lead to gene loss (Panchy et al., 2016). Indeed, the microsyntenic block surrounding the *NOOT/NBCL* locus across rosids with a single *NOOT/NBCL* gene, including *C. canadensis* of the Cercidoideae subfamily, is conserved (Figure 7). The syntenic context of *NOOT/NBCL* genes of Papilionoideae species (including *Castanospermum australe*, a basal species in this subfamily) shows similarity with that of rosids with a single *NOOT/NBCL* gene. However, there are some clear differences between the syntenic contexts of the two Papilionoideae *NOOT/NBCL* genes (Figure 7). For example, in all cases, the gene cluster around Papilionoideae *NOOT1/NBCL1* lacks the methyltransferase (shown in light green), the L-gulonolactone oxidase (dark red), and the plant protein of unknown function (cyan). In the Papilionoideae *NOOT2/NBCL2* cluster, other genes are missing in all species, including genes encoding ganglioside-induced differentiation-associated-like protein (tan), chromoplast lycopene beta-cyclase (green), pyrroline-5-carboxylate reductase (yellow), and so on (Figure 7). These results suggest that these genes were rapidly lost after the duplication of the *NOOT/NBCL* region. Subsequently, small changes occurred, which made the clusters become a bit different. For example, the triacylglycerol lipase (purple) and EF-hand calcium binding family protein (blue) genes were lost around the *NOOT1/NBCL1* gene loci of some Papilionoideae sp (e.g., *Lupinus angustifolius NOOT1/NBCL1*; Figure 7). The syntenic context of the two *NOOT/NBCL* genes of Caesalpinioideae species shows a similar pattern of synteny and gene loss. However, their syntenic context is different from that of the Papilionoideae *NOOT/NBCL* regions (Figure 7). This finding, together with the results of phylogenetic analysis, indicates that the ancestral duplication of *NOOT/NBCL* has occurred independently in two nodulating legume subfamilies: the Caesalpinioideae and Papilionoideae.

### Medicago *MtNOOT1* Is Differentially Regulated in Nodule Pericycle Cells Compared with *MtNOOT2* and Parasponia *PanNOOT1*

We demonstrated that in Medicago, *MtNOOT1* is required to suppress cell division in pericycle-derived cells at an early stage of nodule primordium development, whereas such repression does not occur in species that form actinorhizal-type nodules. In line with this observation, we hypothesize that *MtNOOT1* obtained the ability to be expressed in pericycle-derived cells in Medicago nodule primordia to suppress cell division, whereas in actinorhizal-type nodule primordia, *NOOT/NBCL* is not expressed in pericycle-derived cells during nodule formation. We studied the expression patterns of *NOOT* genes in Medicago and Parasponia nodule primordia by *in situ* hybridization, since no functional promoters (that can complement the *Mtnoot1* phenotype) could be obtained for GUS reporter studies (we tested the up to 5-kb upstream region before the start codon of *MtNOOT1*). The hybridization probe sets contained ~20 adjacent oligonucleotide pairs of 20 nucleotides long probes that hybridize to specific regions within the target mRNA (see Methods). In Medicago nodule primordia, *MtNOOT1* and *MtNOOT2* were expressed in the nodule meristem and (young) infected cells (Figures 8C and 8D). Furthermore, *MtNOOT1* was expressed in pericycle-derived cells, whereas *MtNOOT2* was not (Figures 8E and 8F; Supplemental Figure 8). Parasponia *PanNOOT1* transcripts were predominately detected in the nodule meristem and infected cells of the primordia, (like *MtNOOT1* and *MtNOOT2*) but were barely detectable in dividing pericycle cells (Figures 8G and 8H). These results suggest that in Medicago, the *cis*-regulatory elements of *MtNOOT1* and *MtNOOT2* diverged and that MtNOOT1 has (neo) functionalized to allow expression in pericycle-derived cells of the nodule primordia. Such expression is essential for suppressing the development of actinorhizal-type nodules in this legume species, suggesting that actinorhizal-type nodules are ancestral and that legume-type legumes are derived.

## DISCUSSION

Actinorhizal-type nodules have been described as modified lateral roots originating from the root pericycle, like lateral roots (Pawlowski and Bisseling, 1996; Huss-Danell, 1997; Pawlowski and Demchenko, 2012; Svistoonoff et al., 2014; Ibáñez et al., 2017). However, we demonstrated that during actinorhizal-type nodule formation, the cells derived from the (parental) root cortex specifically form the tissue containing the intracellularly hosted nitrogen-fixing microsymbionts. This is very similar to legume nodule formation, in which the infected central tissue is also derived from mitotically activated root cortex cells (Xiao et al.,

**Figure 2.** (continued).

**(C)** and **(I)** Anticlinal divisions are induced in the endodermis (arrows). **(I)** UV light image of the endodermis region as indicated by the red box in the section shown in **(C)**. Mitotically active endodermis cells lost Casparian strips.

**(D)** and **(E)** Cell divisions continue in inner cortical cells (C3 to C4), forming multiple cell layers, and pericycle-derived cells form a dome-shaped structure. **(E)** and **(F)** Pericycle-derived cells start to form nodule vascular tissues. Root endodermis-derived cells, which appear light blue after toluidine blue staining, flank the pericycle-derived nodule vasculature. At the apex of the vascular bundle, root endodermis-derived cells remain undifferentiated (without Casparian strips, see **[J]**). Cells derived from C3 to C4 are infected by *Frankia*; see arrowheads in **(F)** and the red boxed region in **(E)**.

**(G)** Infected cortical cells become part of the mature nodule lobe. A group of dividing cells at the tip of nodule vasculature appears to form a nodule lobe meristem (M).

**(J)** and **(K)** UV light images of root endodermis regions of the nodules shown in **(E)** and the red boxed region shown in **(G)**, respectively. Root endodermis-derived cells at the apex of the nodule vasculature remain undifferentiated. Root endodermis cells in the peripheral region of the nodule vasculature have lignified cell walls, as indicated by arrows in **(J)** and **(K)**. Dotted line marks the border between endodermis- and pericycle-derived cells. ep, Epidermis; C1-C4, four cortical cell layers; ed, endodermis; pc, pericycle. Scale bars, 50 μm (**[A]** to **[E]** and **[G]** to **[K]**), 25 μm **(F)**.

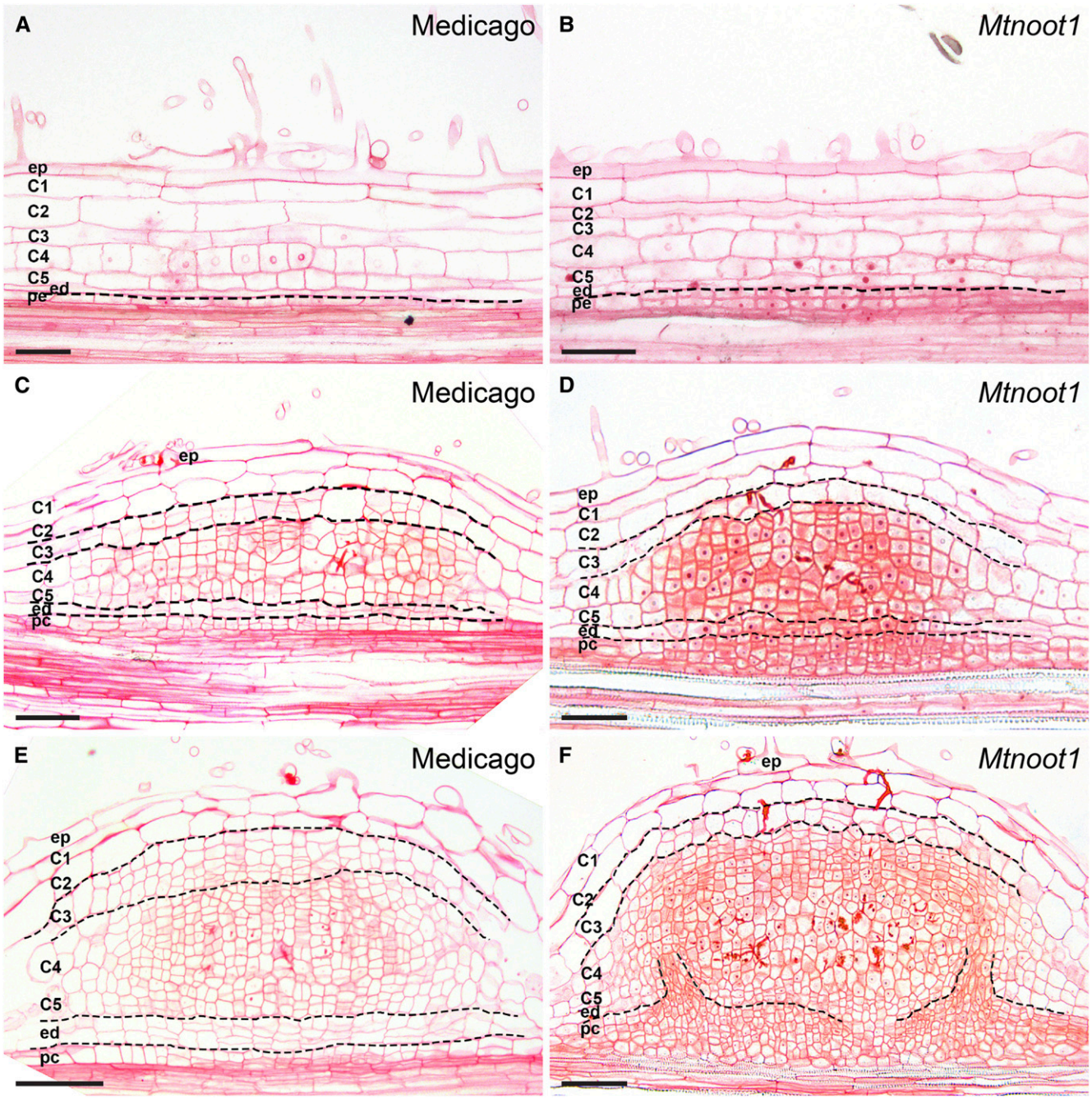


**Figure 3.** Pericycle- and Endodermis-Derived Cells in *Mtnoot1* Nodule Primordia Remain Mitotically Active.

**(A)** to **(F)** Three subsequent stages of wild-type Medicago nodule primordia (**[A]**, **[C],** and **[E]**), compared with similar developmental stages of *Mtnoot1* nodule primordia (tnk507;**[B]**, **[D],** and **[F]**), respectively. **(A)** and **(B)** The mitotic activity of pericycle-derived cells is more active in *Mtnoot1* **(B)**. **(C)** and **(D)** Pericycle- and endodermis-derived cells form four to six cell layers in wild type **(C)** and six to eight cell layers in *Mtnoot1* nodule primordia **(D)**. The number of periclinal divisions is markedly higher in *Mtnoot1* **(D)**. **(E)** and **(F)** Pericycle- and endodermis-derived cells stop dividing in wild-type nodule primordia **(E)**; however, they maintain their mitotic activity in *Mtnoot1* **(F)**. **(C)** to **(F)** Fewer cell layers are derived from the middle cortex (C3) in *Mtnoot1* nodule primordia (**[D]** and **[F]**) compared with wild-type Medicago nodule primordia (**[C]** and **[E]**). Dotted lines mark the border between different cell types. ep, Epidermis; C1-C5, five cortical cell layers; ed, endodermis; pc, pericycle. Scale bars, 50 μm.

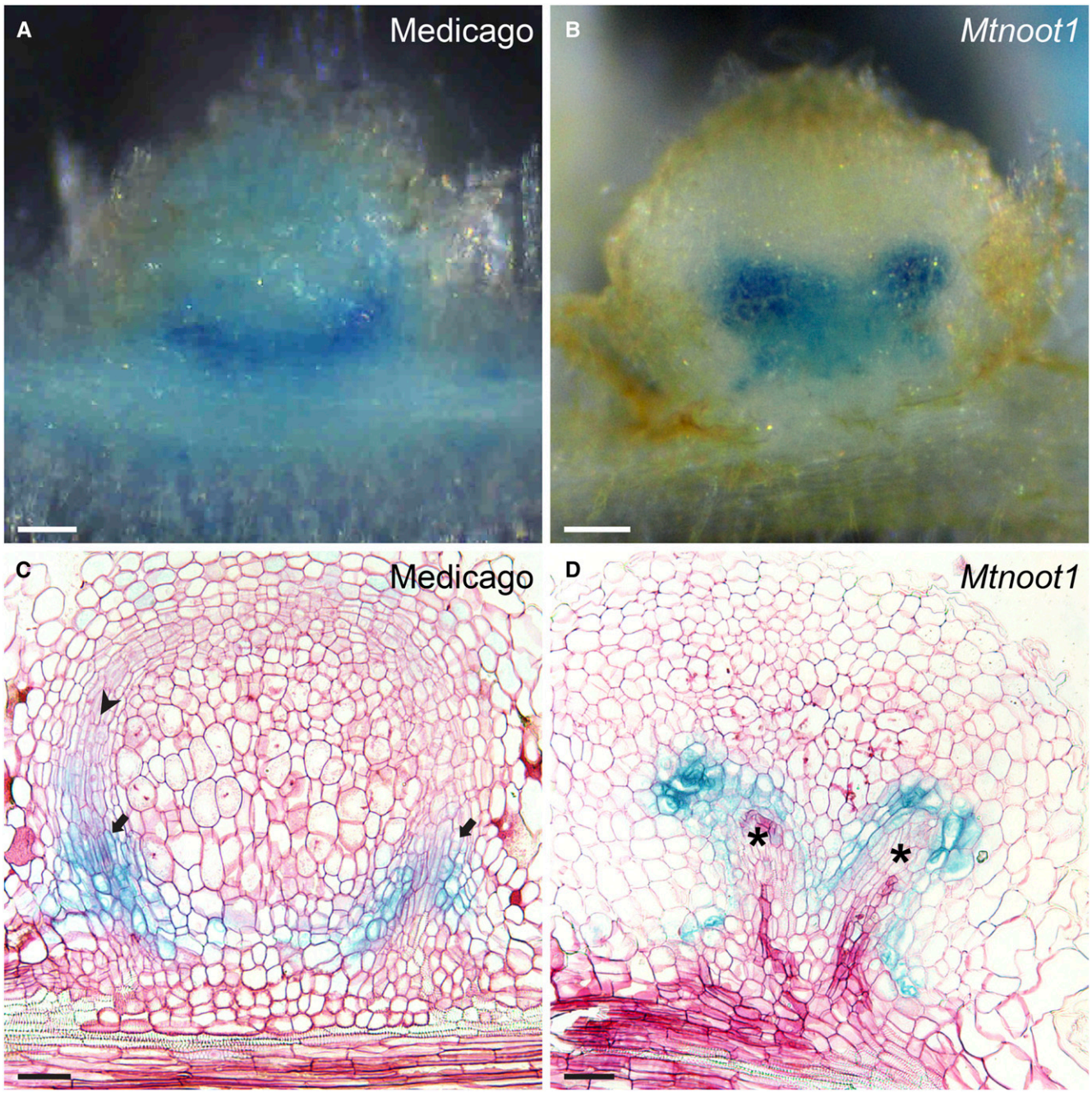


**Figure 4.** The Ontogeny of the Medicago *Mtnoot1* Mutant Is Similar to That of Actinorhizal-Type Nodules.

Longitudinal sections of transgenic nodules (14 dpi) expressing *ProAtCASP1:GUS* in wild-type Medicago (**[A]** and **[C]**) and *Mtnoot1* (tnk507; **[B]** and **[D]**).
**(A)** and **(B)** Whole-mount views of the nodules whose sections are shown in **(C)** and **(D)**, respectively.
**(A)** and **(C)** In wild-type nodules, *ProAtCASP1:GUS* is mainly expressed in the newly formed endodermis cells of the nodule vascular bundles (arrows). These cells develop from root cortex-derived cells. Young developing vascular cells have an elongated shape (arrowhead).
**(B)** and **(D)** In *Mtnoot1*, GUS activity occurs in the most distal cells of the developing nodule vascular bundles (*). These cells are derived from the root endodermis. At the proximal part of the nodule vasculature, a new endodermis formed in which *ProAtCASP1:GUS* is expressed.
**(A)** to **(D)** Representative results from three independent experiments, in which 26 *Mtnoot1* nodules with *ProAtCASP1:GUS* expression in endodermis-derived cells were sectioned, 13 of which exhibited the phenotype as shown in **(D)**. Serial sections were produced, and only the section containing the tip of nodule vasculature is shown in **(C)** and **(D)**. In **(D)**, the tip of the vasculature on the right side is shown. Scale bar, 50 μm (**[A]** and **[B]**), 100 μm (**[C]** and **[D]**).

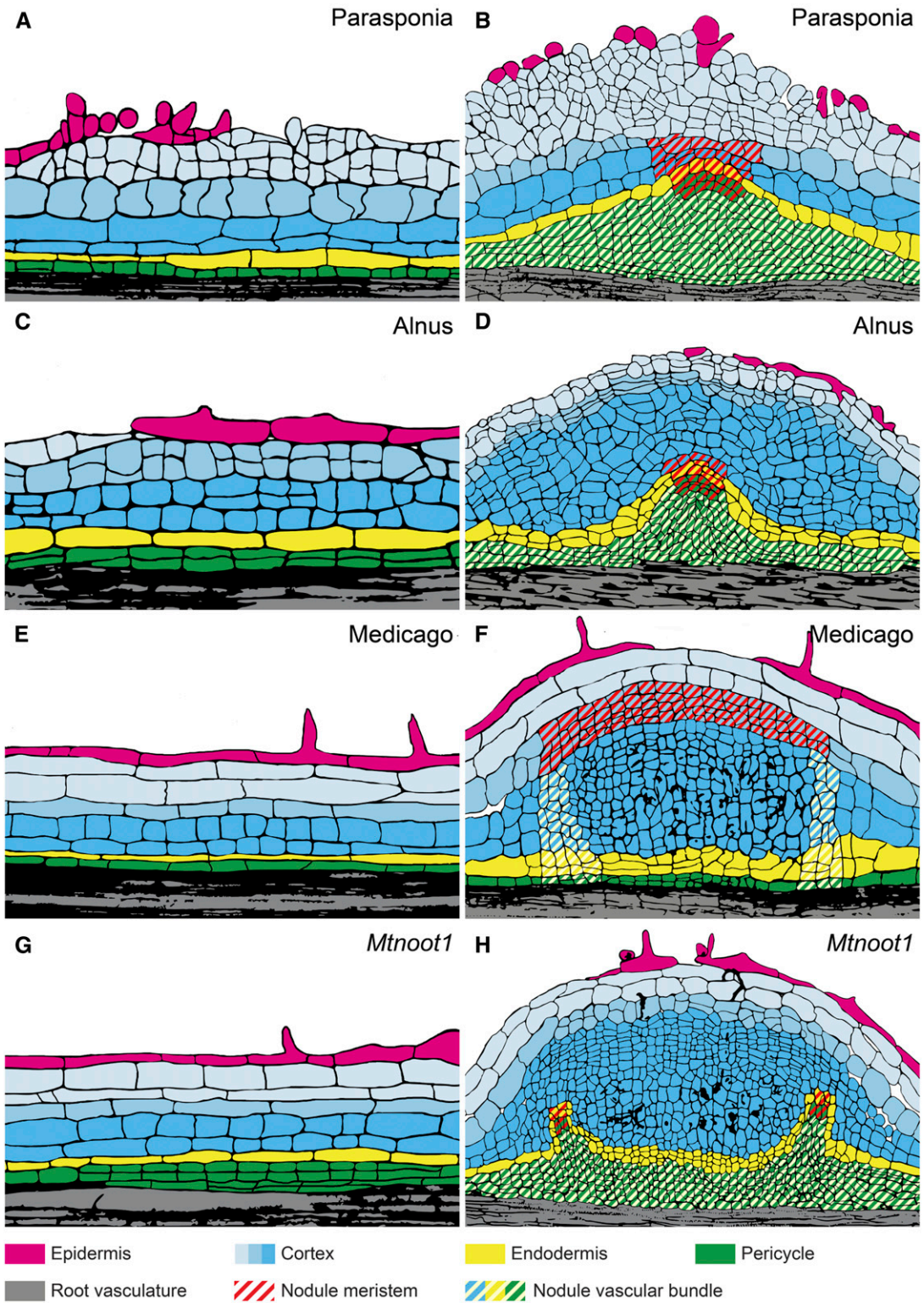


**Figure 5.** Fate Maps of Actinorhizal-Type and *Mtnoot1* Nodules.

**(A)** to **(H)** Two nodule primordium stages of Parasponia (**[A]** and **[B]**), Alnus (**[C]** and **[D]**), wild-type Medicago (**[E]** and **[F]**), and *Mtnoot1* (**[G]** and **[H]**). **(B)**, **(D)**, **(F)**, and **(H)** In all cases, cortex-derived cells are colonized by infection threads containing bacteria. These infected cells become part of the mature nodule.

**(B)**, **(D)**, and **(H)** The ontogeny of the nodule vascular bundle is similar in actinorhizal-type nodules (**[B]** and **[D]**) and in *Mtnoot1* **(H)**. Color and pattern legends are shown at the bottom.

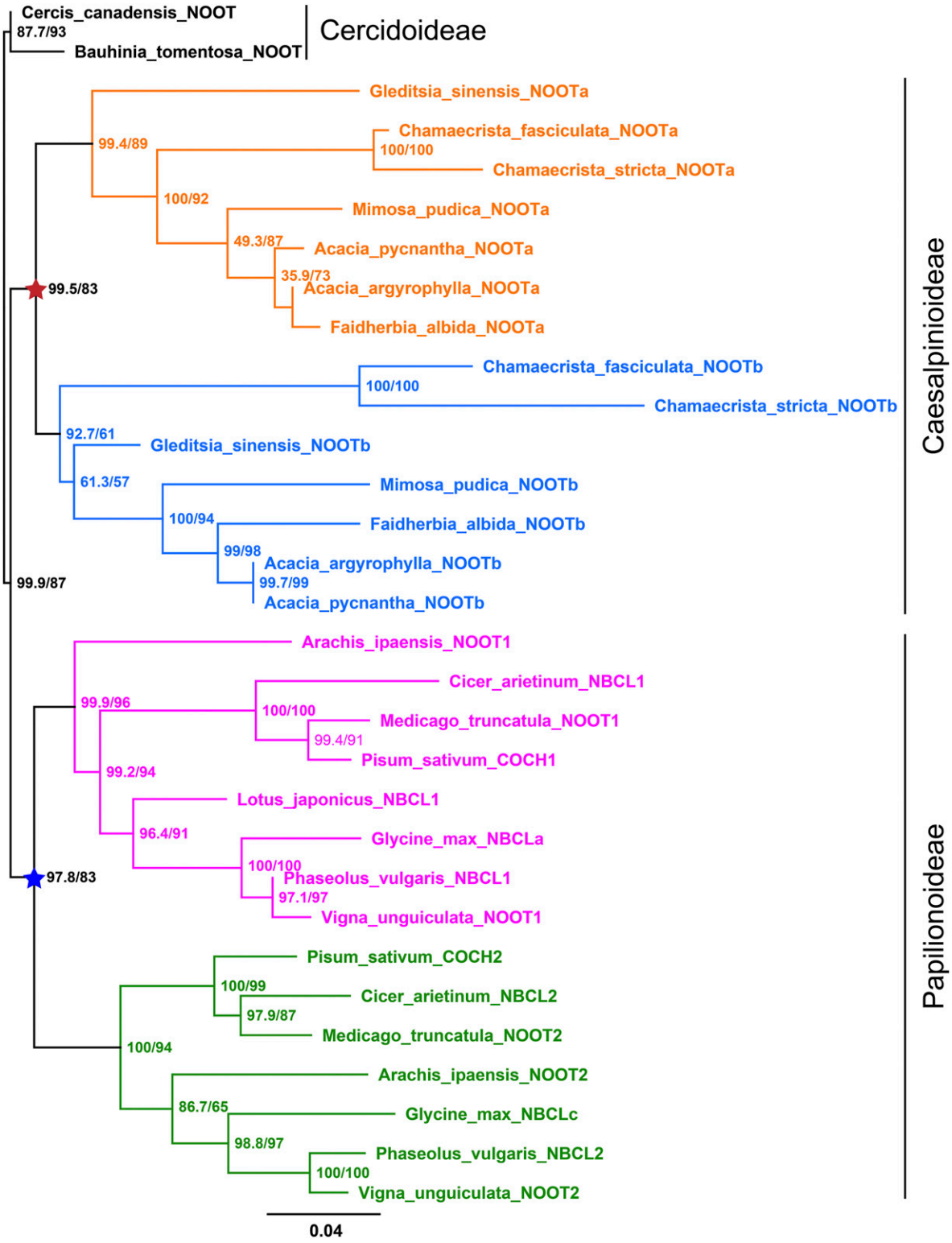


**Figure 6.** Maximum Likelihood Tree of Legume NOOT/NBCL Proteins.

The NOOT/NBCL proteins are present in three legume subfamilies, with Cercidoideae representing the most basal one. The Cercidoideae family members for which sequence data are available, *Cercis canadensis* and *Bauhinia tomentosa*, do not form nodules and contain a single *NOOT/NBCL* gene. Except for *Lotus japonicus* and *Glycine max*, all other legumes (subfamilies Papilionoideae and Caesalpinioideae) for which sequence data are available have two

2014). This led us to conclude that the ontogenies of legume and actinorhizal-type nodules are much more similar than previously proposed. Furthermore, we showed that legume-type nodules can be (partially) converted to actinorhizal-type nodules by knocking out a *NOOT/NBCL* gene, i.e., *MtNOOT1* in Medicago, suggesting that legume-type nodules might have evolved from actinorhizal-type nodules. This supports the hypothesis that nodulation evolved only once in a common ancestor of the NFC. Furthermore, our study provides circumstantial evidence that the actinorhizal nodule type is ancestral.

Nodule formation involves processes that have been co-opted from the more ancient arbuscular mycorrhizal (AM) symbiosis. For example, in both legume and actinorhizal plants, the signaling pathway that is essential for nodule formation is (in part) shared with that activated by AM fungi (reviewed in Markmann and Parniske, 2009; Oldroyd et al., 2011; Geurts et al., 2012). Furthermore, in Medicago, the same exocytosis pathway is used for the intracellular hosting of rhizobia as well as AM fungi (Ivanov et al., 2012). Here, we revealed an additional commonality, because in both nodule and AM symbiosis, the root cortex (-derived tissue) is exclusively used to host the microsymbiont. A difference between these two types of symbiosis is that bacterial infection involves mitotically activated cortical cells, whereas AM fungi enter "existing" cortical cells. However, it was recently suggested that cell division-related processes also occur in cortical cells during the accommodation of AM fungi (Russo et al., 2019).

A major difference between legume-type and actinorhizal-type nodules lies in the ontogeny and position of the nodular vascular bundles (Figure 5). In actinorhizal-type nodules, the vascular bundles are derived from the pericycle, whereas in legume-type nodules, they are derived from cortical cells. Furthermore, the vasculature has a central position in actinorhizal-type nodules, whereas they are located at the periphery of legume-type nodules. A loss-of-function mutation in Medicago *MtNOOT1* caused a switch from legume- to actinorhizal-type ontogeny of the nodule vasculature (Figure 5). Whether such a switch of nodule ontogeny occurs in other legume *noot1/nbcl1* mutants (e.g., *Pscoch1* mutants) remains to be tested.

We previously showed that nodule primordia formed by the Medicago *lumpy infections* (*lin*) mutant can form small vasculature derived from pericycle cells (Xiao et al., 2014). *MtLIN* encodes a predicted E3 ubiquitin ligase required for infection thread formation. *Mtlin* mutants only form small nodule primordia with very few cortex-derived cells (Kuppusamy et al., 2004; Kiss et al., 2009; Guan, 2013; Liu, 2019a). However, the number of cell layers derived from the pericycle is higher in these mutants than in wild-type primordia. Therefore, the formation of vasculature from pericycle cells corresponds with the increased mitotic activity in these cells, like in the *Mtnoot1* mutant. The *Mtnoot1* phenotype exhibits a stronger shift toward the actinorhizal-type nodules than the *Mtlin* phenotype, as *Mtnoot1* mutant nodules are larger and contain fully infected cells, and roots can grow out at their apex. The *Mtnoot1* mutation did not result in the presence of the vasculature in a central position of the nodule. However, vasculature can originate from a central position in the mutant but still "migrate" to the periphery of the nodule (Figure 4D). In actinorhizal-type nodules, the vasculature is positioned between clusters of dividing cells. We hypothesize that the cortical cell divisions that occur during legume nodule primordium formation are more organized, by which only a single cluster of cells is formed and the vasculature can only obtain a peripheral position.

*Mtnoot2* mutants do not form nodules with root outgrowths. However, the occurrence of nodule roots increases in *Mtnoot1 Mtnoot2* double mutants (Magne et al., 2018a). Therefore, MtNOOT2 also plays a role in maintaining nodule organ identity. Medicago *MtNOOT1*, *MtNOOT2*, and Parasponia *PanNOOT1* are orthologous to the Arabidopsis paralogous genes *BLADE-ON-PETIOLE1* (*AtBOP1*) and *AtBOP2*. These Arabidopsis genes are involved in the formation of boundaries between the shoot apical meristem and lateral organs by suppressing cell division (reviewed by Aida and Tasaka, 2006; Khan et al., 2014; Žádníková and Simon, 2014; Hepworth and Pautot, 2015; Wang et al., 2016). Knockout of *AtBOP1* and *AtBOP2* disrupts organ boundary patterning, causing the loss of leaf abscission, leafy petioles, fused inflorescence, and so on (Ha et al., 2003, 2004; Hepworth et al., 2005; McKim et al., 2008). The general function of *AtBOP1* and *AtBOP2* is to suppress cell division to form a boundary between two groups of cells with different fates (the shoot apical meristem versus lateral organs). This is consistent with the function of *MtNOOT1* in Medicago nodule primordia, where it suppresses the mitotic activity of pericycle- and endodermis-derived cells. This causes a boundary to form between the infected tissue and the root vasculature. In contrast to its paralog *MtNOOT2* and the single-copy ortholog *PanNOOT1*, *MtNOOT1* is expressed in pericycle-derived cells of the nodule primordium. This suggests that the *cis*-regulatory elements of *MtNOOT1* have neofunctionalized to allow *MtNOOT1* to be expressed in these cells, thereby suppressing the development of actinorhizal-type nodule vasculature.

We also showed that the duplication of *NOOT/NBCL* genes most likely occurred independently in the root of the Papilionoideae subfamily and that of the Caesalpinioideae subfamily. Both Papilionoideae and Caesalpinioideae species form legume-type nodules (Elliott, 2007; Santos et al., 2017). One of the most

**Figure 6.** (continued).

*NOOT/NBCL* genes that are grouped into four major clades, with two clustered clades containing Papilionoideae *NOOT/NBCL* genes (indicated in pink and green) and the other clades containing Caesalpinioideae *NOOT/NBCL* genes (indicated in orange and blue). This suggests that the *NOOT/NBCL* gene was independently duplicated in the common ancestor of Papilionoideae (blue star) and in that of Caesalpinioideae (red star). Numbers at the nodes indicate approximate Bayes support (%)/ultrafast bootstrap support (%). Ultrafast bootstrap approximation values are based on 5000 replicates. The protein sequences used in this analysis are summarized in Supplemental Table 1. For convenience, previously unnamed NOOT/NBCL proteins were all named NOOT in this analysis. *Glycine max* NBCLb (Glyma19g131000.1) is a truncated protein and was therefore not included in this analysis. *C. canadensis* and *B. tomentosa* from the Cercidoideae subfamily are the two most basal legumes in the analysis; therefore, *C. canadensis* NOOT and *B. tomentosa* NOOT were used as the outgroup. Branch lengths were scaled (see the bottom) and represent the number of substitutions per site. Note that the asterisks are shown in the same color and position as in Supplemental Figure 1.

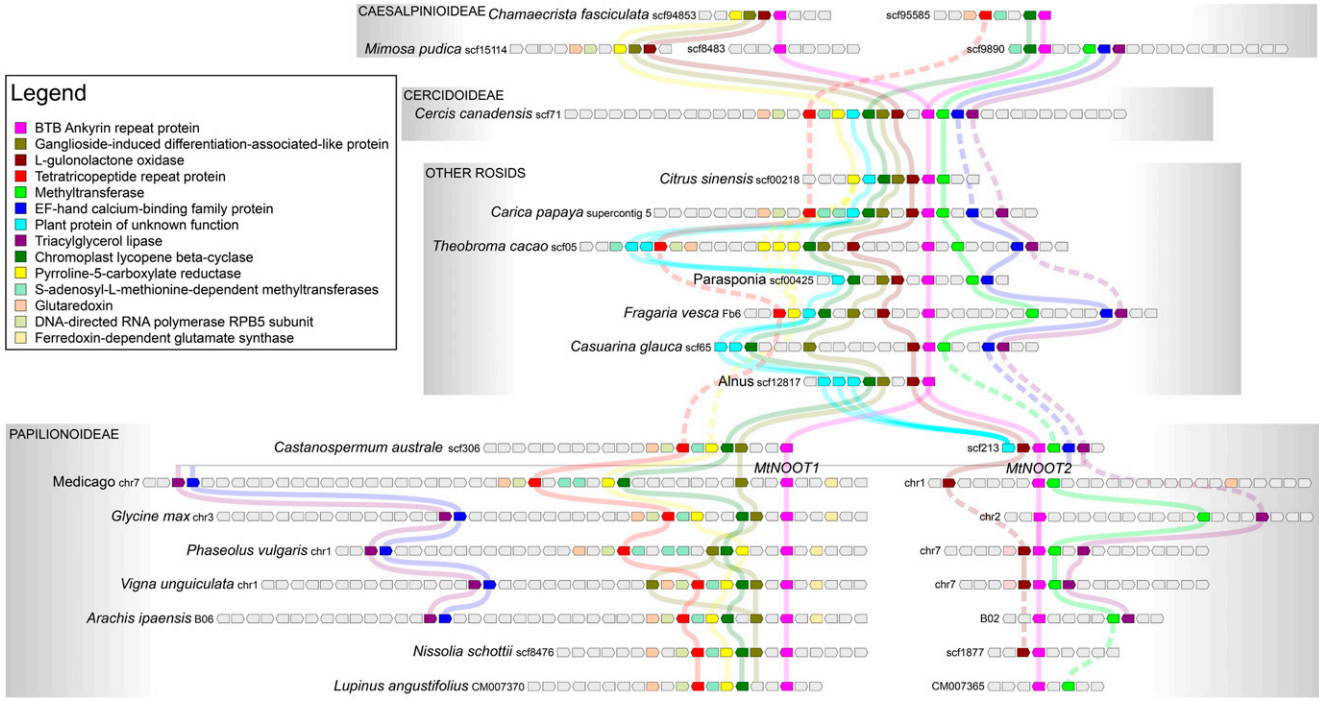


**Figure 7.** Independent Duplication of *NOOT/NBCL* Genomic Region in Legumes.

*NOOT/NBCL* (pink block) is part of a block of microsynteny (different colored blocks) across the rosids shown here, including *Citrus sinensis* (Sapindales), *Carica papaya* (Brassicales), *Theobroma cacao* (Malvales), Parasponia (Rosales), *Fragaria vesca* (Rosales), *Casuarina glauca* (Fagales, actinorhizal plant), and Alnus (Fagales). These species were selected because they have only a single *NOOT/NBCL* gene, which seems to represent the ancestral microsyntenic block of *NOOT/NBCL* genes. In the basal legume subfamily Cercidoideae, the microsyntenic block of the *Cercis canadensis NOOT/NBCL* gene is conserved as in the other rosids. In other legumes (subfamilies Papilionoideae and Caesalpinioideae), this entire block was duplicated, giving rise to the paralogs *NOOT1/NBCL1* and *NOOT2/NBCL2*. In Papilionoideae (*Castanospermum australe*, Medicago, *Glycine max*, *Phaseolus vulgaris*, *Vigna unguiculata*, *Arachis ipaensis*, *Nissolia schottii*, *Lupinus angustifolius*), the gene context of *NOOT1/NBCL1* and *NOOT2/NBCL2* (including *C. australe*, a sister species to all other Papilionoideae species) shows similarity with that of rosids, with one copy of the *NOOT/NBCL* gene. However, the gene context of the two Papilionoideae *NOOT/NBCL* genes is clearly different. For example, the genes encoding methyltransferase (light green), L-gulonolactone oxidase (dark red), and plant protein of unknown function (cyan) were lost in all case around the gene locus of Papilionoideae *NOOT1/NBCL1*. Around the gene locus of Papilionoideae*NOOT2/NBCL2,* genes encoding the ganglioside-induced differentiation-associated-like protein (tan), chromoplast lycopene beta-cyclase (green), and pyrroline-5-carboxylate reductase (yellow) are absent. Most likely this is due to the independent loss of different surrounding genes after the duplication of the *NOOT/NBCL* genomic region in the common ancestor of Papilionoideae, after which the gene composition was maintained. The gene context of the two Caesalpinioideae (*Chamaecrista fasciculata* and *Mimosa pudica*) also shows similarity with that of rosids, with a single *NOOT/NBCL* gene. However, the gene context of the two Caesalpinioideae *NOOT/NBCL* genes is different from that of Papilionoideae *NOOT/NBCL* genes; different genes were lost around the gene locus of the two Caesalpinioideae *NOOT/NBCL* genes. Together with phylogenetic analysis, microsynteny analysis suggests that the *NOOT/NBCL* genomic region was duplicated independently in the common ancestor of Papilionoideae and that of Caesalpinioideae. *Pisum sativum COCH1* (*PsCOCH1*), *PsCOCH2*, and *Lotus japonicus NBCL1* (*LjNBCL1*) were not included in the microsynteny analysis, because the *P. sativum* genome is not yet well annotated and three loci of the *LjNBCL1* gene with identical nucleotide sequence are present in the *L. japonicus* genome. The functions of the genes represented by colored blocks are indicated in the inserted legend.

important outcomes of gene duplication is the origin of novel functions (Zhang, 2003). Therefore, the evolutionary trajectory of *NOOT/NBCL* in legumes suggests that the altered *cis*-regulatory elements of *MtNOOT1*, which control gene expression in pericycle-derived cells, might widely occur in legumes. The evolution of regulatory sequences is often the basis for the evolution of form (Carroll, 2005). Therefore, the proposed neofunctionalization of the *cis*-regulatory elements of legume *NOOT/NBCL* might represent a significant evolutionary step toward the evolution of the legume-type nodule. Since the duplication of *NOOT/NBCL* in Papilionoideae might have occurred independently from that in Caesalpinioideae, it is likely that the evolution of legume-type nodule is to some extent independent (but convergent) in Caesalpinioideae. To verify this notion, functional analysis of Caesalpinioideae *NOOT/NBCL* genes should be performed in the future.

## METHODS

### Plant Materials and Growth Conditions

Parasponia (*Parasponia andersonii*) line WU1-14 tissue culture plants were generated as previously described by Op den Camp et al. (2011). Plantlets were grown at 28°C under a 16-h-light/8-h-dark photoperiod. Plantlets were spot inoculated on the root tip region with *Bradyrhizobium elkanii* WUR3 (Op den Camp et al., 2012) after 2 weeks of growth in square Petri

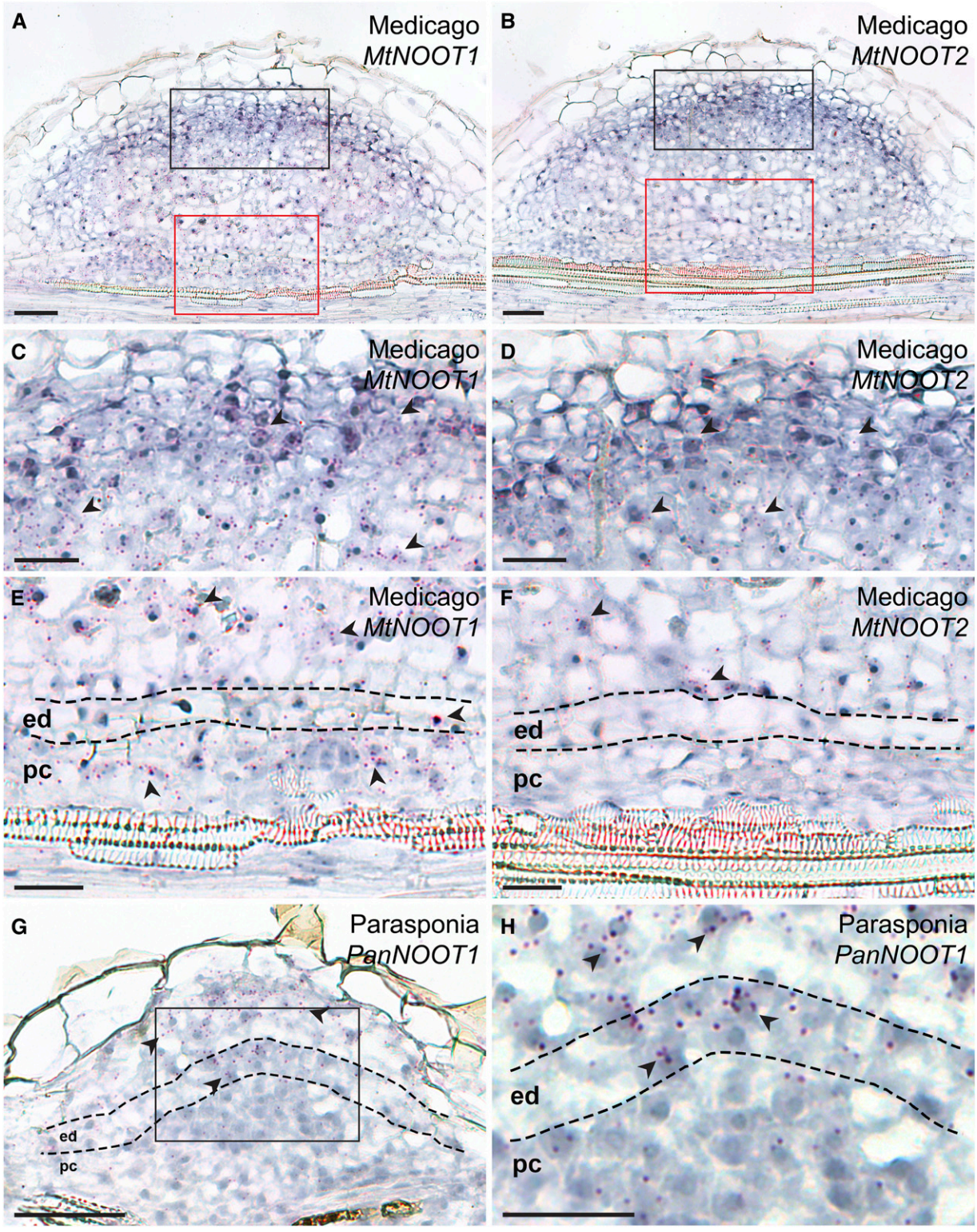


**Figure 8.** The Expression Patterns of *MtNOOT1*, *MtNOOT2*, and *PanNOOT1* in Nodule Primordia.

**(A)** and **(B)** Adjacent sections of a single Medicago nodule primordium, showing the expression pattern of *MtNOOT1* and *MtNOOT2*, respectively.
**(C)** and **(E)** The black and red boxed region in the section shown in **(A)**, respectively.
**(D)** and **(F)** The black and red boxed region in the section shown in **(B)**, respectively.

dishes on EKM medium with low nitrate (0.02 mM $NH_4NO_3$) contents (Becking, 1983). After inoculation, the position of the root tip was marked, and only the root segments (~0.5 cm) above the mark were sampled. Root segments were harvested 7, 10, 18, and 20 d postinoculation. Root segments containing lateral root primordia were harvested from plantlets grown for 2 weeks on EKM without inoculation.

Alnus (*Alnus glutinosa*) seeds were obtained from Svenska Skogsplantor. For surface sterilization, the seeds were washed with 0.2% (w/v) SDS in a 2-mL Eppendorf tube for 10 min in a water sonicator and incubated in 70% (v/v) ethanol for 5 min prior to treatment with concentrated $H_2SO_4$ for 3 to 4 min. The Alnus seeds were rinsed twice with sterile double-distilled water and sterilized with 7% (w/v) NaClO in 0.1% (w/v) SDS for 30 min on a rotary shaker at 150 rpm at room temperature. The sterilized seeds were washed five times with sterile double-distilled water. Alnus seedlings were grown in square Petri dishes or in sand with 0.25-strength Hoagland's medium (Hoagland and Arnon, 1939) under a 16-h-light (26°C)/8-h-dark (24°C) photoperiod. Alnus seeds were germinated in square Petri dishes with slope agar containing 0.8% (w/v) agar and 0.25 Hoagland's with 10 mM $KNO_3$ covered with a piece of nylon mesh (pore size 16 μm; Bigman). When the root systems had reached a few cm in length, the mesh plus plantlets was transferred to a square Petri dish with slope agar based on 0.25 Hoagland's without $KNO_3$. The root tip regions of seedlings in square Petri dishes were spot inoculated with *Frankia alni* ACN14a Normand at al., 2007 grown in basic propionate medium (Benoist et al., 1992). After inoculation, the position of the root tip was marked, and only the root segments (~0.5 cm) above the mark were sampled. Root segments were harvested at 10, 12, and 21 d postinoculation. Seedlings in sand were inoculated with *Frankia alni* ACN14a grown in basic propionate medium, and root segments were harvested at 17 and 28 d postinoculation. Root segments containing lateral root primordia were harvested from plants grown in sand without inoculation.

Plants of the Medicago (*Medicago truncatula*) *noot1* mutant lines tnk507 and NF2717 (Couzigou, 2012) and wild-type accession R108 were grown in square Petri dishes with buffered nodulation medium (supplemented with 1 mM amino ethoxyvinylglycine) at 21°C under a 16-h-light/8-h-dark photoperiod to study Medicago nodule development. Tnk507 and R108 were also used to generate *ProAtCASP1:GUS* transgenic roots via *Agrobacterium rhizogenes* (strain MSU440)-mediated transformation as previously described by Xiao et al. (2014) and Limpens et al. (2004). Each independent experiment contained at least 20 plants per genotype. The *ProAtCASP1:GUS* construct is derived from (Roppolo et al., 2011). The *AtCASP1* promoter region comprised the 1207-bp region before the start codon of *AtCASP1* (AT2G36100). Transgenic plants used for GUS analysis were grown in perlite saturated with nitrogen-free Fahraeus solution at 21°C under a 16-h-light/8-h-dark photoperiod. *Sinorhizobium meliloti* Rm41 (Szende and Ördögh, 1960) carrying the pHC60-GFP construct was used to induce Medicago nodule formation. Medicago seeds were surface-sterilized and germinated as previously described byLimpens et al. (2004).

### Microscopy and Imaging

Root segments and nodules were fixed overnight in 4% paraformaldehyde (w/v), 5% glutaraldehyde (v/v) in 0.05 M sodium phosphate buffer (pH 7.2) at 4°C. The fixed material was dehydrated in an ethanol series and embedded in Technovit 7100 (Heraeus Kulzer) according to the manufacturer's protocol. Sections (7 to 12 μm) were cut with a RJ2035 microtome (Leica Microsystems) and stained for 1.5 min in 0.05% (w/v) toluidine blue O to analyze lateral root and nodule development or 10 min in 0.1% (w/v) ruthenium red to examine transgenic GUS material. The sections were analyzed under a DM5500B microscope equipped with a DFC425C camera (Leica Microsystems). In the fate maps of Parasponia and Alnus nodule development, we used Casparian strips—the hallmark of the endodermis—to trace endodermis development. The cells derived from the pericycle and cortex are positioned below and above the endodermis-derived cells, respectively. The sections were larger than those shown in the figures to allow the root layer from which they originate to be traced back easily. To observe Casparian strips, the sections were analyzed under a SP8 confocal microscope (Leica) or a LSM 710 confocal laser-scanning microscope (Zeiss).

### Microsynteny Analysis

To assess the microsyntenic context of *NOOT/NBCL* within rosids, we selected the following genomes from the legume family, irrespective of *NOOT/NBCL* copy number: from Cercidoideae, *Cercis canadensis* (doi: 10.5524/101044;) from Caesalpinioideae, *Chamaecrista fasciculata* (doi: 10.5524/101045) and *Mimosa pudica* (doi: 10.5524/101049;) from Papilionoideae: *Castanospermum australe* (kindly provided by Henk Hilhorst), *Arachis ipaensis* (https://peanutbase.org), *Nissolia schottii* (doi: 10.5524/101050), *Lupinus angustifolius* (NCBI: GCA_001865875.1), Medicago, soybean (*Glycine max*), common bean (*Phaseolus vulgaris*), and cowpea (*Vigna unguiculata*). We selected the following genomes from other rosids based on the finding that they contain a single putative *NOOT/NBCL* ortholog, and it is therefore likely that they retained an ancestral microsyntenic pattern: from Malvids, cocoa tree (*Theobroma cacao*), papaya (*Carica papaya*), and *Citrus sinensis*; from Fabids, wild strawberry (*Fragaria vesca*), Alnus (http://gigadb.org/dataset/101042), *Casuarina glauca* (http://gigadb.org/dataset/101051), and Parasponia (parasponia.org). All genomes were downloaded from Phytozome v12 unless indicated otherwise. Putative orthologous genes were identified based on phylogenetic analysis of aligned predicted proteins using MAFFT v7.388 (Katoh et al., 2002) with default parameter settings (auto algorithm; scoring matrix, BLOSUM62; gap opening penalty, 1.53; offset value, 0.123), and FastTree 2.1.5 (Price et al., 2010) with default parameter settings (rates categories of sites, 20), implemented in Geneious R8 (Biomatters).

### Phylogenetic Analysis

Information about the protein sequences used for phylogenetic analysis is summarized in the Supplemental Table. For phylogenetic analysis, full-length or partial (predicted) protein sequences were aligned using MAFFT v7.429 (https://mafft.cbrc.jp/alignment/server/; Katoh et al., 2002, 2019) with default parameter settings (auto algorithm; scoring matrix, BLOSUM62; gap opening penalty, 1.53; offset value: 0). The alignment was curated using trimAl v1.4.1 (https://ngphylogeny.fr/tools/tool/284/form;

**Figure 8.** (continued).

**(A)**, **(C)**, and **(E)** *MtNOOT1* is expressed in the developing nodule meristem and infected cells **(C)**. *MtNOOT1* is also expressed in the pericycle- and endodermis-derived cells in nodule primordia **(E)**.

**(B)**, **(D)**, and **(F)** *MtNOOT2* is expressed in the developing nodule meristem and infected cells **(D)**, but not in the pericycle- or endodermis-derived cells in nodule primordia **(F)**.

**(G)** and **(H)** *PanNOOT1* transcripts are predominately present in the infected cells and developing nodule meristem but barely detectable in the pericycle-derived cells in nodule primordia. **(H)** A magnification of the boxed region in **(G)**. Red dots represent mRNA transcripts, and some are indicated by arrowheads. Dotted line marks the border between different cell types. ed, Endodermis; pc, pericycle. Scale bars, 50 μm (**[A]**, **[B],** and **[G]**), 25 μm (**[C]** to **[F]**, and **[H]**).

Capella-Gutiérrez et al., 2009), with default parameter settings (gap threshold, automatic; similarity threshold, automatic; consistency threshold, automatic; Supplemental File 1). Curated alignment was used for tree building using W-IQ-TREE (Trifinopoulos et al., 2016) with the best-fit substitution model (Kalyaanamoorthy et al., 2017). Branch support analysis was performed using ultrafast bootstrap approximation based on 5000 replicates (Minh et al., 2013) and approximate Bayes test (Anisimova et al., 2011). The tree was rooted on *Cercis canadensis* NOOT and *Bauhinia tomentosa* NOOT, as *C. canadensis* and *B. tomentosa* are the two most basal legume species in the analysis. A machine-readable tree file is provided in Supplemental File 2.

### *In Situ* Hybridization

For sample preparation, Medicago R108 plants were grown as described above and nodule primordia were collected at 5 d postinoculation. Parasponia tissue culture plants were grown for 10 d in perlite saturated with EKM solution and inoculated with *Mesorhizobium plurifarium* BOR2 as previously described by van Zeijl et al. (2018) and Wardhani et al. (2019). Hybridization were performed using Invitrogen ViewRNA ISH tissue 1-plex assay kits (Thermo Fisher Scientific), as previously described by Liu et al. (2019b). For the user manual, see https://assets.thermofisher.com/TFS-Assets/LSG/manuals/MAN0018633_viewRNA_ISH_UG.pdf. Modifications were as follows: section thickness was 6 μm; Silane-prep slides (Sigma-Aldrich) were used to increase the adhesion of the sections to the slides. The probe sets for *MtNOOT1* (catalog no. VF1-16434), *MtNOOT2* (catalog no.VF1-6001055), and *PanNOOT1* (catalog no. VF1-6000669) were designed and synthesized by Thermo Fisher Scientific. *MtNOOT1* probe sets cover the 2-913 nucleotide region of the coding sequence (1449 nucleotides, Medtr7g090020.1); *MtNOOT2* probe sets cover the 1024-2221 nucleotide region of the full-length mRNA (2537 nucleotides, XM_013611955); and *PanNOOT1* probe sets cover the 281-1146 nucleotide region of the coding sequence (1512 nucleotides, PanWU01x14_292800.1). A typical probe set contained ~20 oligonucleotide pairs of probes that hybridize to specific regions across the target mRNA. Each probe covers 20 nucleotides, and only a pair of two adjacent probes, which target a 40-nucleotide-long sequence, can form a site for signal amplification. This allows the background to be reduced, eliminating the need for control probes. Sections were imaged as mentioned above.

### Accession Numbers

Sequence data from this article are listed in the Supplemental Table.

### Supplemental Data

**Supplemental Figure 1.** NFC.

**Supplemental Figure 2.** Parasponia lateral root developmental stages.

**Supplemental Figure 3.** Alnus lateral root developmental stages.

**Supplemental Figure 4.** Casparian strips reform in the peripheral region of root endodermis-derived cells, but not in the central region.

**Supplemental Figure 5.** The Casparian strips of Alnus nodule vascular endodermis cells form at a later stage of development.

**Supplemental Figure 6.** Pericycle- and endodermis-derived cells remain mitotically active in *Mtnoot1* (NF2717) nodule primordia.

**Supplemental Figure 7.** The expression of *ProAtCASP1:GUS* in endodermis-derived cells in nodule primordia.

**Supplemental Figure 8.** *MtNOOT2* is not expressed in pericycle-derived cells in nodule primordia.

**Supplemental Table.** Protein sequences used in the phylogenetic analysis.

**Supplemental File 1.** Curated alignment of legume NOOT/NBCL protein sequences.

**Supplemental File 2.** Maximum likelihood tree file of legume NOOT/NBCL proteins.

## ACKNOWLEDGMENTS

We thank Pascal Ratet for providing the *Mtnoot1* seeds (tnk507 and NF2717) and Niko Geldner for providing the *AtCASP1* promoter GUS fusion vector. We also thank Henk Hilhorst for providing access to the unpublished genome of *Castanospermum australe* and Wouter Kohlen for providing access to the unpublished transcriptome of *Chamaecrista stricta*. This research was supported by the European Research Council (grant ERC-2011-AdG294790 to T.B.); the Swedish Research Council Vetenskapsrådet (grant VR 2012-03061 to K.P.); the Netherlands Organization for Scientific Research (grant 865.13.001 to R.G.) and the China Scholarship Council (grant 201306040120 to D.S.).

## AUTHOR CONTRIBUTIONS

T.B. conceived the project; T.B. and K.P. designed the experiments; D.S. and T.T.X. performed most of the experiments with help from X.G.; R.v.V. performed the microsynteny analysis; O.K. and D.S. performed *in situ* hybridization; D.S. and T.B. wrote the article with input from R.v.V., R.G., and K.P.

Received October 21, 2019; revised March 30, 2020; accepted April 9, 2020; published April 10, 2020.

## REFERENCES

**Aida, M., and Tasaka, M.** (2006). Genetic control of shoot organ boundaries. Curr. Opin. Plant Biol. **9:** 72–77.

**Anisimova, M., Gil, M., Dufayard, J.-F., Dessimoz, C., and Gascuel, O.** (2011). Survey of branch support methods demonstrates accuracy, power, and robustness of fast likelihood-based approximation schemes. Syst. Biol. **60:** 685–699.

**Becking, J.H.** (1983). The *Parasponia parviflora*-Rhizobium symbiosis. Host specificity, growth and nitrogen fixation under various conditions. Plant Soil **75:** 309–342.

**Benoist, P., Müller, A., Diem, H.G., and Schwencke, J.** (1992). High-molecular-mass multicatalytic proteinase complexes produced by the nitrogen-fixing actinomycete *Frankia* strain BR. J. Bacteriol. **174:** 1495–1504.

**Berg, R.H., Langenstein, B., and Silvester, W.B.** (1999). Development in the *Datisca-Coriaria* nodule type. Can. J. Bot. **77:** 1334–1350.

**Bonnett, H.T., Jr.** (1969). Cortical cell death during lateral root formation. J. Cell Biol. **40:** 144–159.

**Burgess, D., and Peterson, R.L.** (1987). Development of *Alnus japonica* root nodules after inoculation with *Frankia* strain HFPArI3. Can. J. Bot. **65:** 1647–1657.

**Callaham, D., and Torrey, J.G.** (1977). Prenodule formation and primary nodule development in roots of *Comptonia* (Myricaceae). Can. J. Bot. **55:** 2306–2318.

**Capella-Gutiérrez, S., Silla-Martínez, J.M., and Gabaldón, T.** (2009). trimAl: A tool for automated alignment trimming in large-scale phylogenetic analyses. Bioinformatics **25:** 1972–1973.

**Carroll, S.B.** (2000). Endless forms: The evolution of gene regulation and morphological diversity. Cell **101:** 577–580.

**Carroll, S.B.** (2005). Evolution at two levels: On genes and form. PLoS Biol. **3:** e245.

**Casero, P.J., Casimiro, I., and Lloret, P.G.** (1996). Pericycle proliferation pattern during the lateral root initiation in adventitious roots of *Allium cepa*. Protoplasma **191:** 136–147.

**Couzigou, J.-M., et al.** (2012). *NODULE ROOT* and *COCHLEATA* maintain nodule development and are legume orthologs of *Arabidopsis BLADE-ON-PETIOLE* genes. Plant Cell **24:** 4498–4510.

**Ditta, G., Pinyopich, A., Robles, P., Pelaz, S., and Yanofsky, M.F.** (2004). The *SEP4* gene of *Arabidopsis thaliana* functions in floral organ and meristem identity. Curr. Biol. **14:** 1935–1940.

**Doyle, J.J.** (2011). Phylogenetic perspectives on the origins of nodulation. Mol. Plant Microbe Interact. **24:** 1289–1295.

**Elliott, G.N., et al.** (2007). *Burkholderia phymatum* is a highly effective nitrogen-fixing symbiont of *Mimosa* spp. and fixes nitrogen *ex planta*. New Phytol. **173:** 168–180.

**Fournier, J., et al.** (2018). Cell remodeling and subtilase gene expression in the actinorhizal plant *Discaria trinervis* highlight host orchestration of intercellular *Frankia* colonization. New Phytol. **219:** 1018–1030.

**Franche, C., Lindström, K., and Elmerich, C.** (2009). Nitrogen-fixing bacteria associated with leguminous and non-leguminous plants. Plant Soil **321:** 35–59.

**Garcia-Bellido, A.** (1977). Homoeotic and atavic mutations in insects. Am. Zool. **17:** 613–629.

**Geurts, R., Lillo, A., and Bisseling, T.** (2012). Exploiting an ancient signalling machinery to enjoy a nitrogen fixing symbiosis. Curr. Opin. Plant Biol. **15:** 438–443.

**Griesmann, M., et al.** (2018). Phylogenomics reveals multiple losses of nitrogen-fixing root nodule symbiosis. Science **361:** eaat1743.

**Guan, D., et al.** (2013). Rhizobial infection is associated with the development of peripheral vasculature in nodules of *Medicago truncatula*. Plant Physiol. **162:** 107–115.

**Ha, C.M., Jun, J.H., Nam, H.G., and Fletcher, J.C.** (2004). *BLADE-ON-PETIOLE1* encodes a BTB/POZ domain protein required for leaf morphogenesis in *Arabidopsis thaliana*. Plant Cell Physiol. **45:** 1361–1370.

**Ha, C.M., Kim, G.-T., Kim, B.C., Jun, J.H., Soh, M.S., Ueno, Y., Machida, Y., Tsukaya, H., and Nam, H.G.** (2003). The *BLADE-ON-PETIOLE 1* gene controls leaf pattern formation through the modulation of meristematic activity in *Arabidopsis*. Development **130:** 161–172.

**Hafeez, F., Akkermans, A.D.L., and Chaudhary, A.H.** (1984). Observations on the ultrastructure of *Frankia* sp. in root nodules of *Datisca cannabina* L. Plant Soil **79:** 383–402.

**Hepworth, S.R., and Pautot, V.A.** (2015). Beyond the divide: Boundaries for patterning and stem cell regulation in plants. Front Plant Sci **6:** 1052.

**Hepworth, S.R., Zhang, Y., McKim, S., Li, X., and Haughn, G.W.** (2005). BLADE-ON-PETIOLE-dependent signaling controls leaf and floral patterning in Arabidopsis. Plant Cell **17:** 1434–1448.

**Hoagland, D.R., and Arnon, D.I.** (1939). The water-culture method for growing plants without soil. Calif. Agric. Exp. Stn. Circ. **347:** 1–32.

**Huss-Danell, K.** (1997). Actinorhizal symbioses and their N2 fixation. New Phytol. **136:** 375–405.

**Ibáñez, F., Wall, L., and Fabra, A.** (2017). Starting points in plant-bacteria nitrogen-fixing symbioses: Intercellular invasion of the roots. J. Exp. Bot. **68:** 1905–1918.

**Imanishi, L., Perrine-Walker, F.M., Ndour, A., Vayssières, A., Conejero, G., Lucas, M., Champion, A., Laplaze, L., Wall, L., and Svistoonoff, S.** (2014). Role of auxin during intercellular infection of *Discaria trinervis* by *Frankia*. Front Plant Sci **5:** 399.

**Ivanov, S., Fedorova, E.E., Limpens, E., De Mita, S., Genre, A., Bonfante, P., and Bisseling, T.** (2012). *Rhizobium*-legume symbiosis shares an exocytotic pathway required for arbuscule formation. Proc. Natl. Acad. Sci. USA **109:** 8316–8321.

**Kalyaanamoorthy, S., Minh, B.Q., Wong, T.K.F., von Haeseler, A., and Jermiin, L.S.** (2017). ModelFinder: Fast model selection for accurate phylogenetic estimates. Nat. Methods **14:** 587–589.

**Katoh, K., Misawa, K., Kuma, K., and Miyata, T.** (2002). MAFFT: A novel method for rapid multiple sequence alignment based on fast Fourier transform. Nucleic Acids Res. **30:** 3059–3066.

**Katoh, K., Rozewicki, J., and Yamada, K.D.** (2019). MAFFT online service: Multiple sequence alignment, interactive sequence choice and visualization. Brief. Bioinform. **20:** 1160–1166.

**Khan, M., Xu, H., and Hepworth, S.R.** (2014). BLADE-ON-PETIOLE genes: Setting boundaries in development and defense. Plant Sci. **215–216:** 157–171.

**Kiss, E., Oláh, B., Kaló, P., Morales, M., Heckmann, A.B., Borbola, A., Lózsa, A., Kontár, K., Middleton, P., Downie, J.A., Oldroyd, G.E.D., and Endre, G.** (2009). LIN, a novel type of U-box/WD40 protein, controls early infection by rhizobia in legumes. Plant Physiol. **151:** 1239–1249.

**Kuppusamy, K.T., Endre, G., Prabhu, R., Penmetsa, R.V., Veereshlingam, H., Cook, D.R., Dickstein, R., and Vandenbosch, K.A.** (2004). *LIN*, a *Medicago truncatula* gene required for nodule differentiation and persistence of rhizobial infections. Plant Physiol. **136:** 3682–3691.

**Lancelle, S.A., and Torrey, J.G.** (1984). Early development of *Rhizobium*-induced root-nodules of *Parasponia rigida*. I. Infection and early nodule initiation. Protoplasma **123:** 26–37.

**Lancelle, S.A., and Torrey, J.G.** (1985). Early development of *Rhizobium*-induced root nodules of *Parasponia rigida*. II. Nodule morphogenesis and symbiotic development. Can. J. Bot. **63:** 25–35.

**Lewis, E.B.** (1963). Genes and developmental pathways. Am. Zoologist **3:** 33–56.

**Limpens, E., Ramos, J., Franken, C., Raz, V., Compaan, B., Franssen, H., Bisseling, T., and Geurts, R.** (2004). RNA interference in *Agrobacterium rhizogenes*-transformed roots of *Arabidopsis* and *Medicago truncatula*. J. Exp. Bot. **55:** 983–992.

**Liu, C.-W., et al.** (2019a). A protein complex required for polar growth of rhizobial infection threads. Nat. Commun. **10:** 2848.

**Liu, J., Rutten, L., Limpens, E., van der Molen, T., van Velzen, R., Chen, R., Chen, Y., Geurts, R., Kohlen, W., Kulikova, O., and Bisseling, T.** (2019b). A remote *cis*-regulatory region is required for *NIN* expression in the pericycle to initiate nodule primordium formation in *Medicago truncatula*. Plant Cell **31:** 68–83.

**Liu, Q.Q., and Berry, A.M.** (1991). The infection process and nodule initiation in the *Frankia*-*Ceanothus* root nodule symbiosis: A structural and histochemical study. Protoplasma **163:** 82–92.

**Lloret, P.G., Casero, P.J., Pulgarini, A., and Navascues, J.** (1989). The behaviour of two cell populations in the pericycle of *Allium cepa*, *Pisum sativum*, and *Daucus carota* during early lateral root development. Ann. Bot. **63:** 465–475.

**LPWG.** (2017). A new subfamily classification of the Leguminosae based on a taxonomically comprehensive phylogeny. Taxon **66:** 44–77.

**Magne, K., et al.** (2018a). *MtNODULE ROOT1* and *MtNODULE ROOT2* are essential for indeterminate nodule identity. Plant Physiol. **178:** 295–316.

**Magne, K., George, J., Berbel Tornero, A., Broquet, B., Madueño, F., Andersen, S.U., and Ratet, P.** (2018b). *Lotus japonicus NOOT-*

*BOP-COCH-LIKE1* is essential for nodule, nectary, leaf and flower development. Plant J. **94:** 880–894.

**Markmann, K., and Parniske, M.** (2009). Evolution of root endosymbiosis with bacteria: How novel are nodules? Trends Plant Sci. **14:** 77–86.

**McKim, S.M., Stenvik, G.-E., Butenko, M.A., Kristiansen, W., Cho, S.K., Hepworth, S.R., Aalen, R.B., and Haughn, G.W.** (2008). The *BLADE-ON-PETIOLE* genes are essential for abscission zone formation in *Arabidopsis*. Development **135:** 1537–1546.

**Miller, I.M., and Baker, D.D.** (1985). The initiation, development and structure of root nodules in *Elaeagnus angustifolia* L. (*Elaeagnaceae*). Protoplasma **128:** 107–119.

**Minh, B.Q., Nguyen, M.A.T., and von Haeseler, A.** (2013). Ultrafast approximation for phylogenetic bootstrap. Mol. Biol. Evol. **30:** 1188–1195.

**Newcomb, W., and Pankhurst, C.E.** (1982). Fine structure of actinorhizal root nodules of *Coriaria arborea* (Coriariaceae). N. Z. J. Bot. **20:** 93–103.

**Normand, P., et al.** (2007). Genome characteristics of facultatively symbiotic *Frankia* sp. strains reflect host range and host plant biogeography. Genome Res. **17:** 7–15.

**Oldroyd, G.E.D., Murray, J.D., Poole, P.S., and Downie, J.A.** (2011). The rules of engagement in the legume-rhizobial symbiosis. Annu. Rev. Genet. **45:** 119–144.

**Op den Camp, R., Streng, A., De Mita, S., Cao, Q., Polone, E., Liu, W., Ammiraju, J.S.S., Kudrna, D., Wing, R., Untergasser, A., Bisseling, T., and Geurts, R.** (2011). LysM-type mycorrhizal receptor recruited for rhizobium symbiosis in nonlegume *Parasponia*. Science **331:** 909–912.

**Op den Camp, R.H.M., Polone, E., Fedorova, E., Roelofsen, W., Squartini, A., Op den Camp, H.J.M., Bisseling, T., and Geurts, R.** (2012). Nonlegume *Parasponia andersonii* deploys a broad rhizobium host range strategy resulting in largely variable symbiotic effectiveness. Mol. Plant Microbe Interact. **25:** 954–963.

**Panchy, N., Lehti-Shiu, M., and Shiu, S.-H.** (2016). Evolution of gene duplication in plants. Plant Physiol. **171:** 2294–2316.

**Parniske, M.** (2018). Uptake of bacteria into living plant cells, the unifying and distinct feature of the nitrogen-fixing root nodule symbiosis. Curr. Opin. Plant Biol. **44:** 164–174.

**Pawlowski, K., and Bisseling, T.** (1996). Rhizobial and actinorhizal symbioses: What are the shared features? Plant Cell **8:** 1899–1913.

**Pawlowski, K., and Demchenko, K.N.** (2012). The diversity of actinorhizal symbiosis. Protoplasma **249:** 967–979.

**Price, M.N., Dehal, P.S., and Arkin, A.P.** (2010). FastTree 2—approximately maximum-likelihood trees for large alignments. PLoS One **5:** e9490.

**Racette, S., and Torrey, J.G.** (1989). Root nodule initiation in *Gymnostoma* (Casuarinaceae) and *Shepherdia* (Elaeagnaceae) induced by *Frankia* strain HFPGpI1. Can. J. Bot. **67:** 2873–2879.

**Roppolo, D., De Rybel, B., Dénervaud Tendon, V., Pfister, A., Alassimone, J., Vermeer, J.E.M., Yamazaki, M., Stierhof, Y.-D., Beeckman, T., and Geldner, N.** (2011). A novel protein family mediates Casparian strip formation in the endodermis. Nature **473:** 380–383.

**Russo, G., Carotenuto, G., Fiorilli, V., Volpe, V., Chiapello, M., Van Damme, D., and Genre, A.** (2019). Ectopic activation of cortical cell division during the accommodation of arbuscular mycorrhizal fungi. New Phytol. **221:** 1036–1048.

**Santi, C., Bogusz, D., and Franche, C.** (2013). Biological nitrogen fixation in non-legume plants. Ann. Bot. **111:** 743–767.

**Santos, J.M., Casaes Alves, P.A., Silva, V.C., Kruschewsky Rhem, M.F., James, E.K., and Gross, E.** (2017). Diverse genotypes of *Bradyrhizobium* nodulate herbaceous *Chamaecrista* (Moench) (Fabaceae, Caesalpinioideae) species in Brazil. Syst. Appl. Microbiol. **40:** 69–79.

**Shubin, N., Tabin, C., and Carroll, S.** (2009). Deep homology and the origins of evolutionary novelty. Nature **457:** 818–823.

**Soltis, D.E., Soltis, P.S., Morgan, D.R., Swensen, S.M., Mullin, B.C., Dowd, J.M., and Martin, P.G.** (1995). Chloroplast gene sequence data suggest a single origin of the predisposition for symbiotic nitrogen fixation in angiosperms. Proc. Natl. Acad. Sci. USA **92:** 2647–2651.

**Sprent, J.I., Sutherland, J.M., de Faria, S.M., Dilworth, M.J., Corby, H.D.L., Becking, J.H., Materon, L.A., and Drozd, J.W.** (1987). Some aspects of the biology of nitrogen-fixing organisms. Philos. Trans. R. Soc. B Biol. Sci. **317:** 111–129.

**Svistoonoff, S., Hocher, V., and Gherbi, H.** (2014). Actinorhizal root nodule symbioses: what is signalling telling on the origins of nodulation? Curr. Opin. Plant Biol. **20:** 11–18.

**Szende, K., and Ördögh, F.** (1960). Die Lysogenie von *Rhizobium meliloti*. Naturwissenschaften **47:** 404–405.

**Torrey, J.G.** (1976). Initiation and development of root nodules of Casuarina (Casuarinaceae). Am. J. Bot. **63:** 335–344.

**Torrey, J.G., and Callaham, D.** (1979). Early nodule development in *Myrica gale*. Bot. Gaz. **140:** S10–S14.

**Trifinopoulos, J., Nguyen, L.T., von Haeseler, A., and Minh, B.Q.** (2016). W-IQ-TREE: A fast online phylogenetic tool for maximum likelihood analysis. Nucleic Acids Res. **44** (W1): W232–W235.

**Valverde, C., and Wall, L.G.** (1999). Time course of nodule development in the *Discaria trinervis* (Rhamnaceae) - *Frankia* symbiosis. New Phytol. **141:** 345–354.

**van Velzen, R., et al.** (2018). Comparative genomics of the nonlegume *Parasponia* reveals insights into evolution of nitrogen-fixing rhizobium symbioses. Proc. Natl. Acad. Sci. USA **115:** E4700–E4709.

**van Velzen, R., Doyle, J.J., and Geurts, R.** (2019). A resurrected scenario: Single gain and massive loss of nitrogen-fixing nodulation. Trends Plant Sci. **24:** 49–57.

**van Zeijl, A., Wardhani, T.A.K., Seifi Kalhor, M., Rutten, L., Bu, F., Hartog, M., Linders, S., Fedorova, E.E., Bisseling, T., Kohlen, W., and Geurts, R.** (2018). CRISPR/Cas9-mediated mutagenesis of four putative symbiosis genes of the tropical tree *Parasponia andersonii* reveals novel phenotypes. Front. Plant Sci. **9:** 1–14.

**Wang, Q., Hasson, A., Rossmann, S., and Theres, K.** (2016). *Divide et impera*: Boundaries shape the plant body and initiate new meristems. New Phytol. **209:** 485–498.

**Wardhani, T.A.K., Roswanjaya, Y.P., Dupin, S., Li, H., Linders, S., Hartog, M., Geurts, R., and van Zeijl, A.** (2019). Transforming, genome editing and phenotyping the nitrogen-fixing tropical Cannabaceae tree *Parasponia andersonii*. J. Vis. Exp. **2019:** 59971.

**Wellmer, F., Graciet, E., and Riechmann, J.L.** (2014). Specification of floral organs in *Arabidopsis*. J. Exp. Bot. **65:** 1–9.

**Xiao, T.T., Schilderink, S., Moling, S., Deinum, E.E., Kondorosi, E., Franssen, H., Kulikova, O., Niebel, A., and Bisseling, T.** (2014). Fate map of *Medicago truncatula* root nodules. Development **141:** 3517–3528.

**Žádníková, P., and Simon, R.** (2014). How boundaries control plant development. Curr. Opin. Plant Biol. **17:** 116–125.

**Zhang, J.** (2003). Evolution by gene duplication: An update. Trends Ecol. Evol. **18:** 292–298.